

Observations of Small-scale Plasma Density Irregularities and Plasma Instability in the Mid-Latitude Ionosphere with SuperDARN HF Radar

J. Michael Ruohoniemi

*Center for Space Science and Engineering Research
Bradley Department of Electrical and Computer Engineering
Virginia Polytechnic Institute and State University (Virginia Tech)
Blacksburg, Virginia USA*

Personal Introduction

- Virginia Tech is the largest research university in the state of Virginia
- Located in the small town of Blacksburg



- I head the SuperDARN HF radar group at Virginia Tech and teach in the Department of Electrical and Computer Engineering
- Four U.S. universities cooperate on the SuperDARN project:
 - Virginia Tech
 - Dartmouth College (New Hampshire)
 - University of Alaska Fairbanks
 - Johns Hopkins University Applied Physics Laboratory (Maryland)

Observations in the Ionosphere with SuperDARN HF Radar

Outline:

Part I Background to the Ionosphere and SuperDARN

Part II Primer on HF radar and coherent backscattering

Part III Expansion of SuperDARN to mid-latitudes

Part IV Ionospheric plasma instabilities

Observations in the Ionosphere with SuperDARN HF Radar

Outline:

Part I Background to the Ionosphere and SuperDARN

Part II Primer on HF radar and coherent backscattering

Part III Expansion of SuperDARN to mid-latitudes

Part IV Ionospheric plasma instabilities

For Young Scientists, consideration of:

- New research capabilities
- Some open questions

Part I Background to the Ionosphere and SuperDARN

- The ionosphere is a weakly ionized plasma, neutral components (molecules, atoms) predominate over ions and electrons
- The dominant source of ions and electrons in the ionosphere is photoionization

Pictured: Airglow from the vicinity of the lower ionosphere that results from the recovery of ionized and excited species. (Photo taken from the International Space Station)



Properties of the Ionosphere

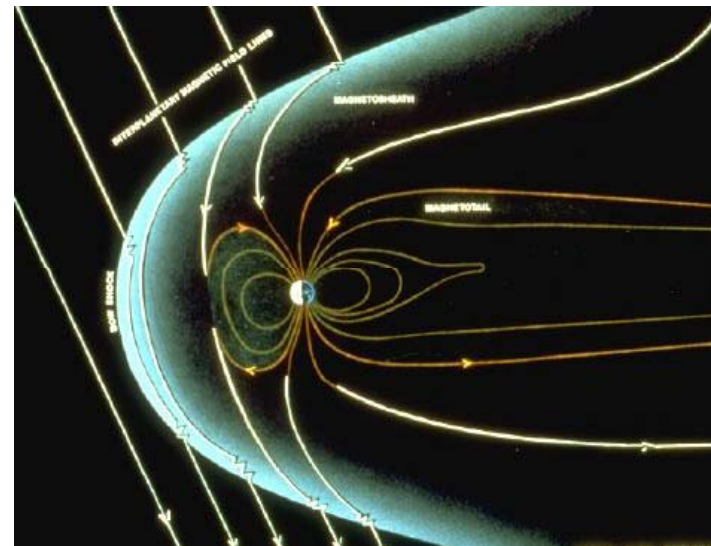
- At high latitudes precipitating particles can be the dominant source through impact ionization (i.e., aurora)



Motion of Charged Particles

- Electric fields, \mathbf{E} , appear in the high-latitude ionosphere due to coupling to the dynamo at the solar wind – magnetosphere boundary
- The coupling is provided by the highly conducting lines of force of the geomagnetic field, \mathbf{B}

Figure: Schematic of solar wind plasma encountering Earth's magnetosphere; electric fields are communicated along the geomagnetic field lines to the high latitude ionosphere

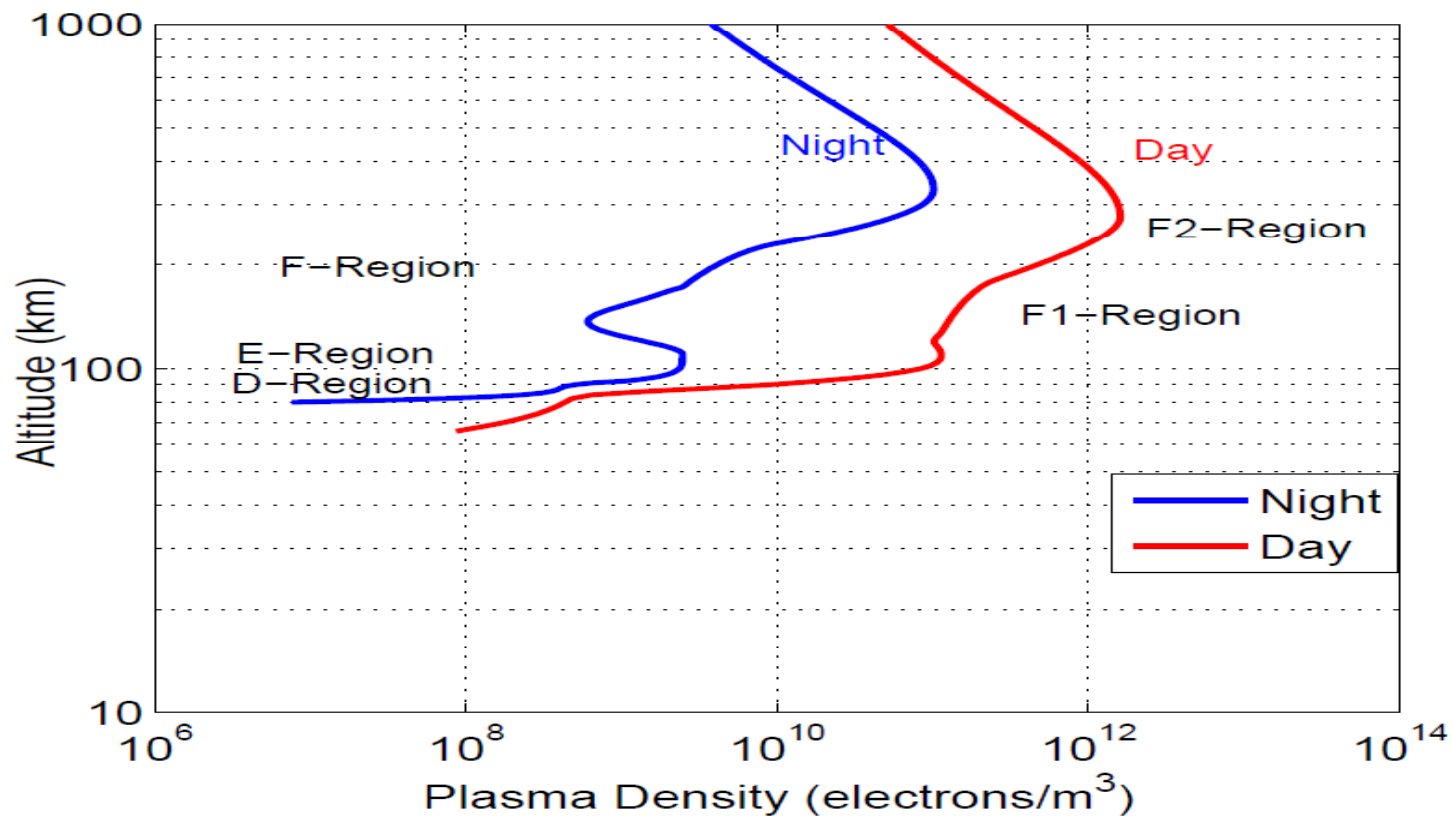


- Note: electric fields can also appear in the ionosphere due to dynamo action of the neutral wind

Regions of the Ionosphere

The ionosphere is generally divided into three major regions based on altitude and the physics that controls the motion of charged particles:

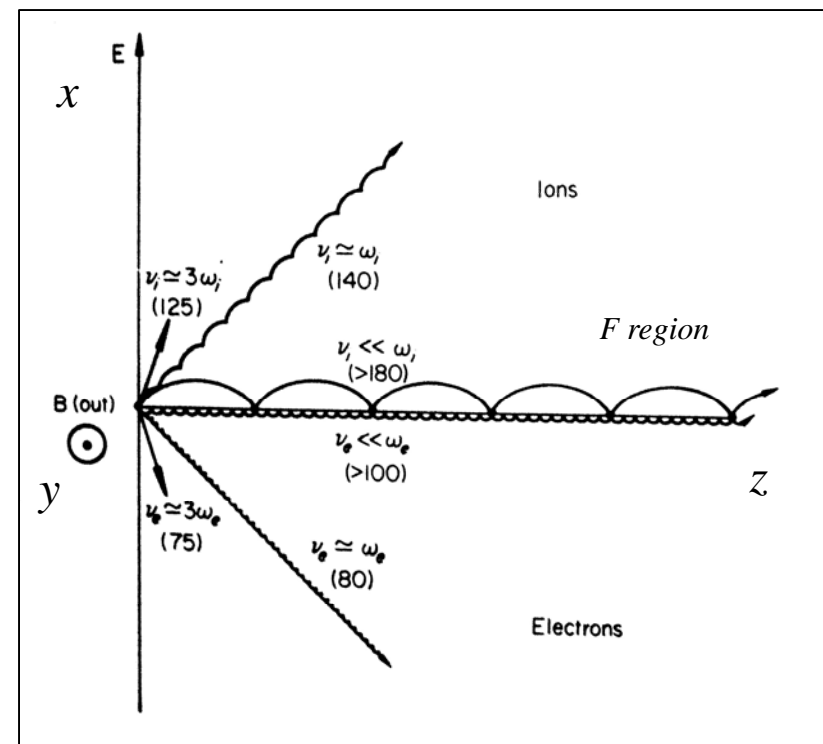
- F-region (150 - 1000 km): both i^+ and e^- controlled by \mathbf{B}
- E-region (90 - 130 km): i^+ controlled by collisions with neutrals, e^- by \mathbf{B}
- D-region (50 - 90 km): both i^+ and e^- controlled by collisions with neutrals



Motion of Charged Particles

- At lower altitudes collisions with neutrals limit the motion of the charged particles
- At higher altitudes the gyration of the charged particles about \mathbf{B} dominates and the resulting motion is in the direction of $\mathbf{E} \times \mathbf{B}$

Figure: Schematic of particle motions for various ratios of collision frequency, ν , and gyrofrequency, ω

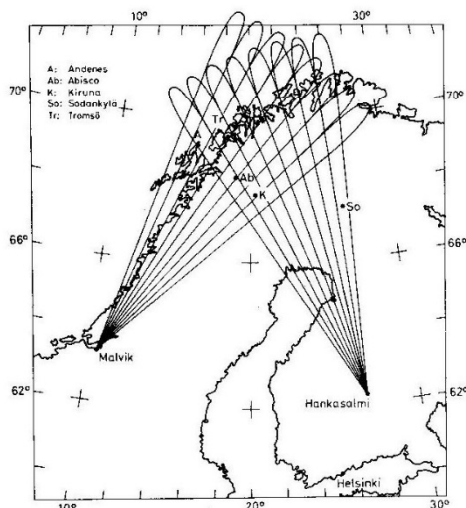


Convection of Plasma in the Ionosphere

- At F region altitudes electric field causes $\mathbf{E} \times \mathbf{B}$ motion of both ions and electrons
- At E region the ions are immobilized by collisions; the differential motion with electrons gives rise to strong electric currents
- $\mathbf{E} \times \mathbf{B}$ motion of the plasma is also called ‘convection’
- Relatively low power coherent scatter radars can measure the motion of the plasma by observing the Doppler shift imposed on backscatter (echoes)
- The backscatter is due to irregularities in plasma density that are carried along by the plasma motion



STARE VHF Radar – E region



- STARE - A bistatic coherent scatter radar built in Scandinavia in the 1970s [Greenwald *et al.*, 1978] and operated at 140 MHz

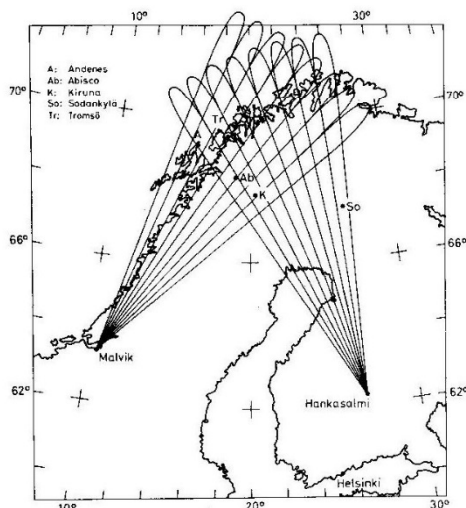
Two receivers were oriented to look over an area of ionosphere and measure backscatter (echoes) from E region plasma within cells defined by beam direction and range gate



STARE receiver array
(Malvik, Norway)

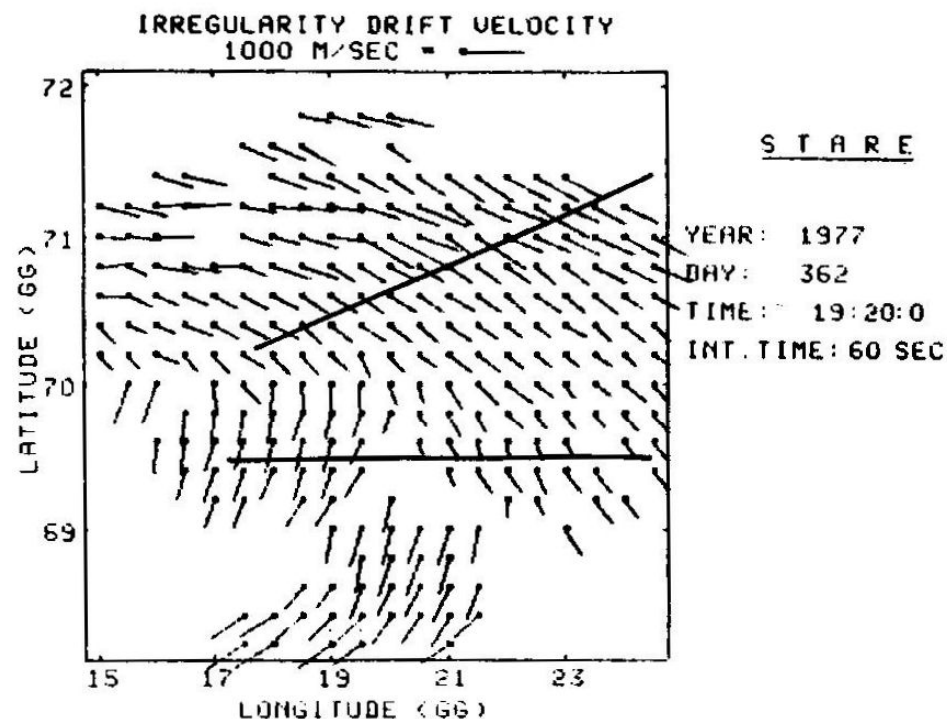


STARE VHF Radar – E region

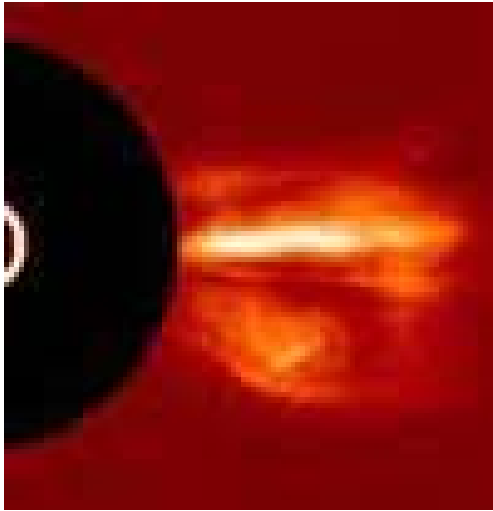


- Map of \mathbf{ExB} plasma velocity inferred from STARE radar measurements, note the high velocity magnitudes (~ 1 km/s)

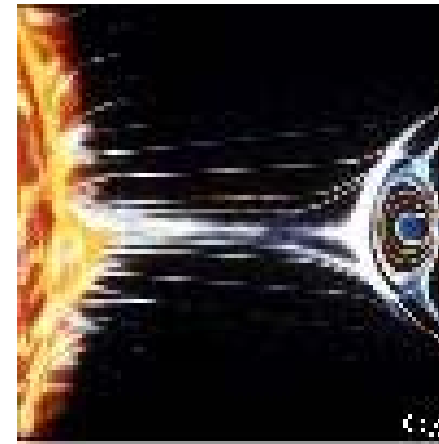
Measurement of the line-of-sight plasma velocities from two directions within the common volumes make it possible to resolve the full 2-dimensional convection velocity vector



Origins of Visual Aurora and Plasma Convection

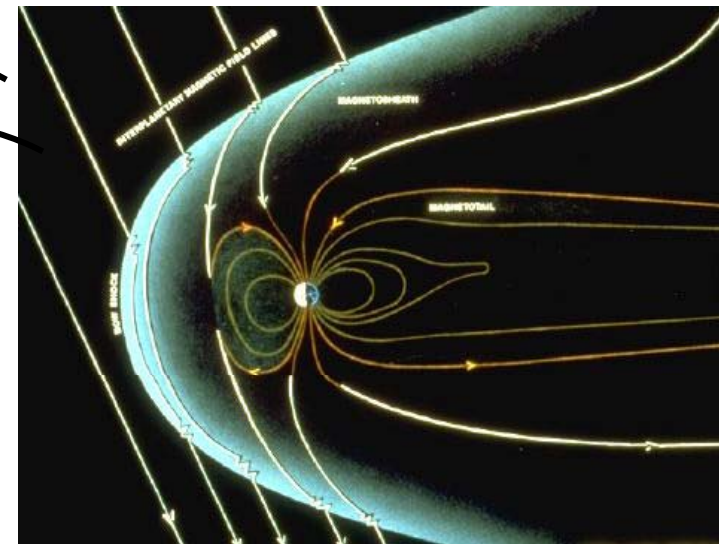
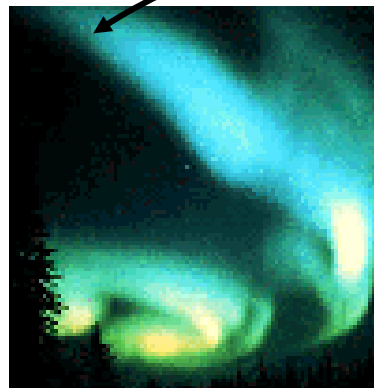
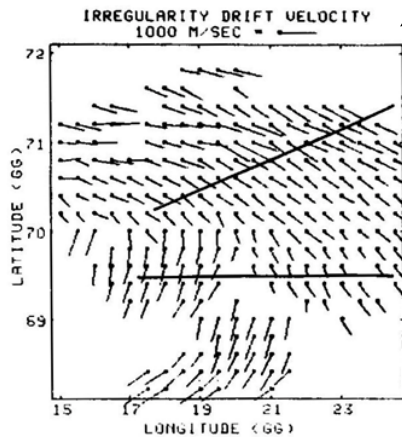


Solar wind plasma
collides with Earth's
magnetosphere



Causing currents
to flow

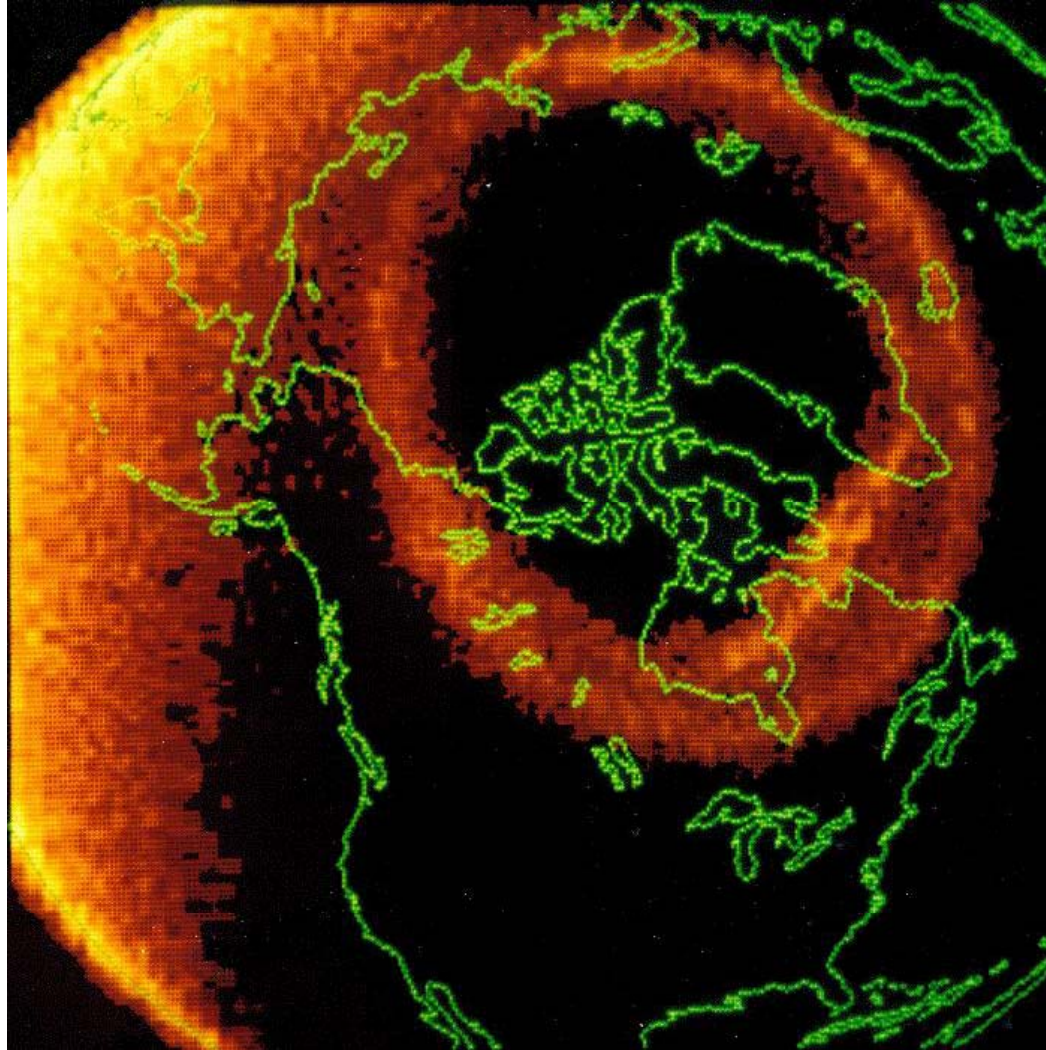
And high-latitude
effects



The Northern Auroral Oval Seen from Space

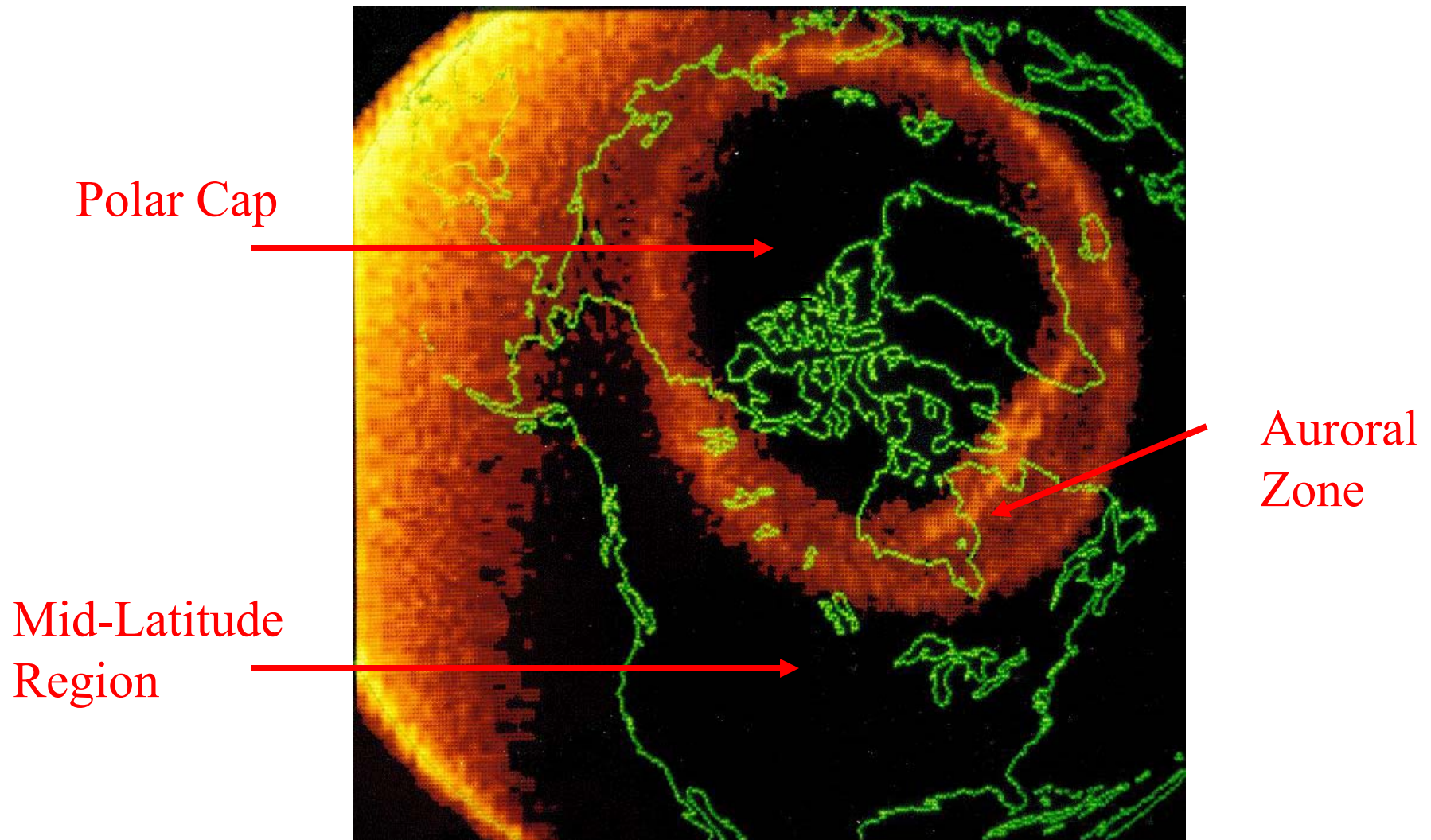
Image of auroral oval taken from the Dynamics Explorer 1 satellite on Nov. 8, 1981

The auroral oval expands and contracts with the level of geomagnetic activity



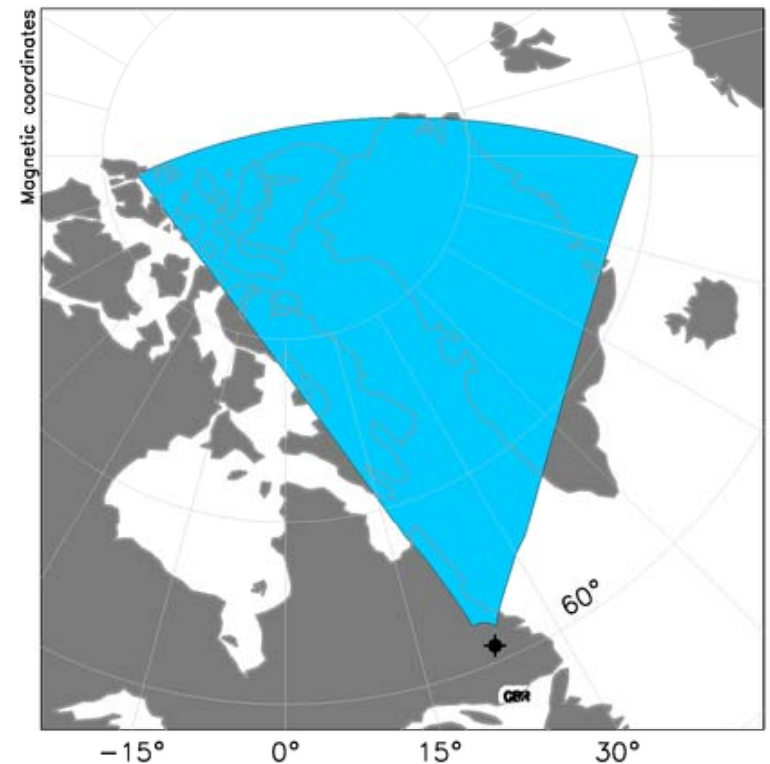
Regions of the High-Latitude Ionosphere

The boundaries of the auroral oval define three regions by geomagnetic latitude



Origins of SuperDARN – 1980s

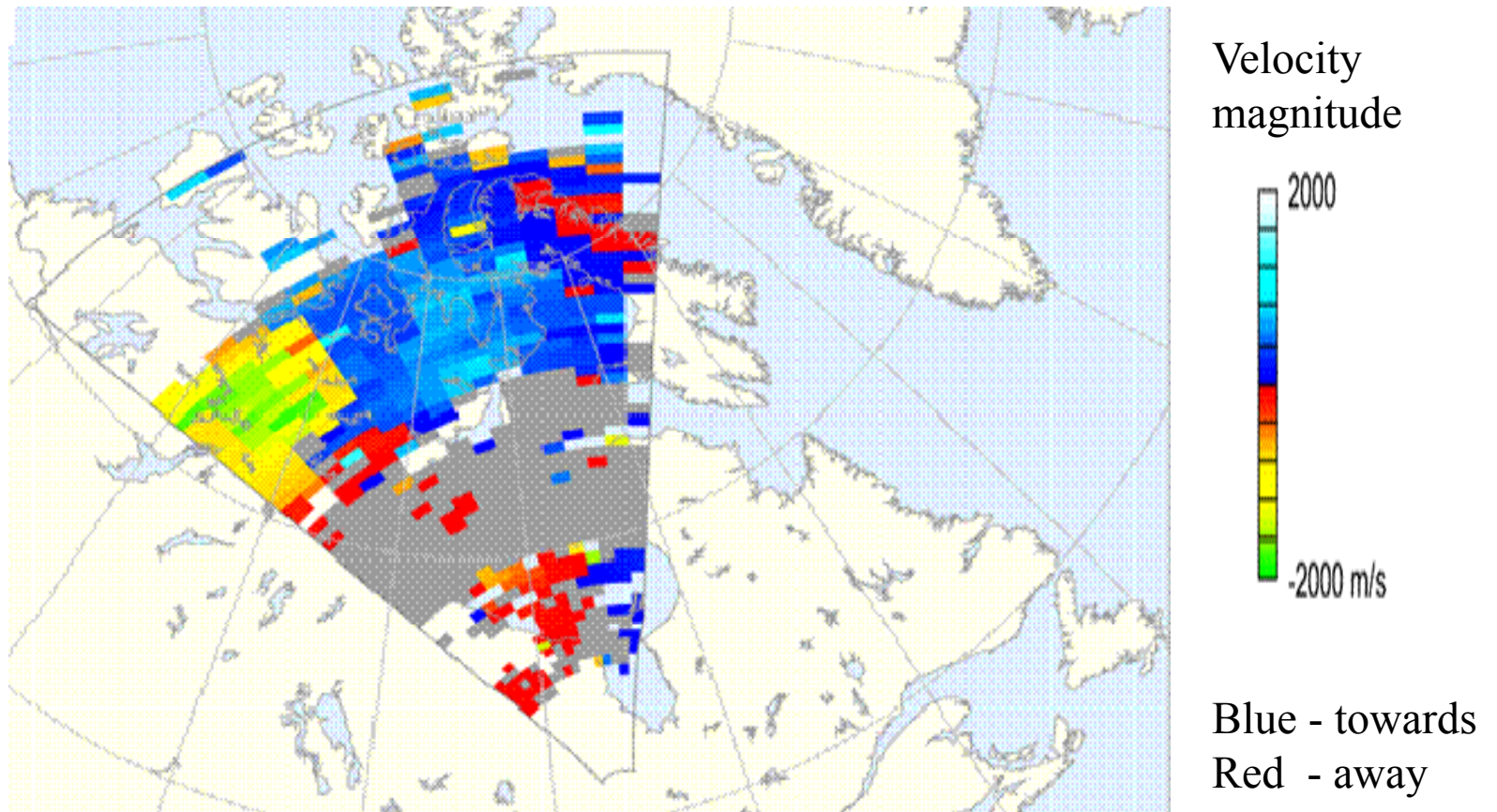
- It was realized that by going to HF frequencies (10-20 MHz) coherent backscatter could be generated
- This greatly increases coverage (to 1000s km range)
- And avoids some issues with the interpretation of E region backscatter



First radar located at Goose Bay, Labrador (Canada)

Observing Plasma Convection in the F region

Map of line-of-sight velocity obtained from a single 2-min radar scan



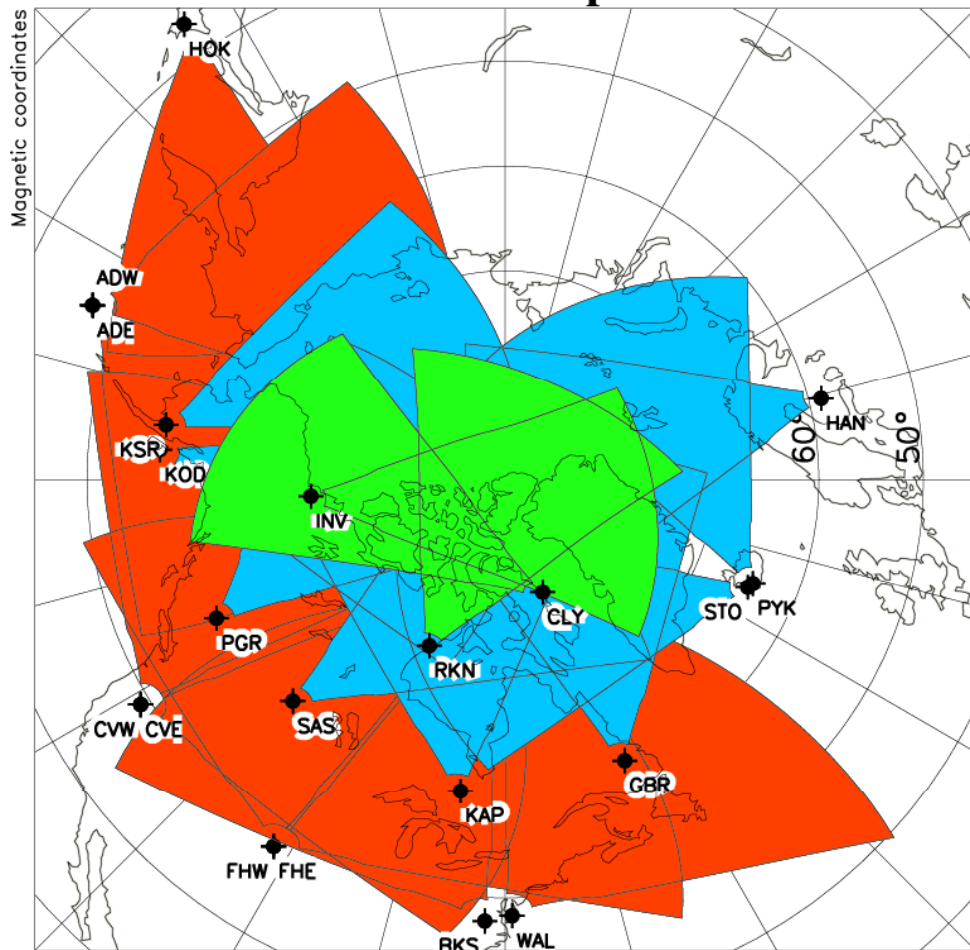
SuperDARN radar located at Kapuskasing, Ontario (Canada)

Brief History of SuperDARN

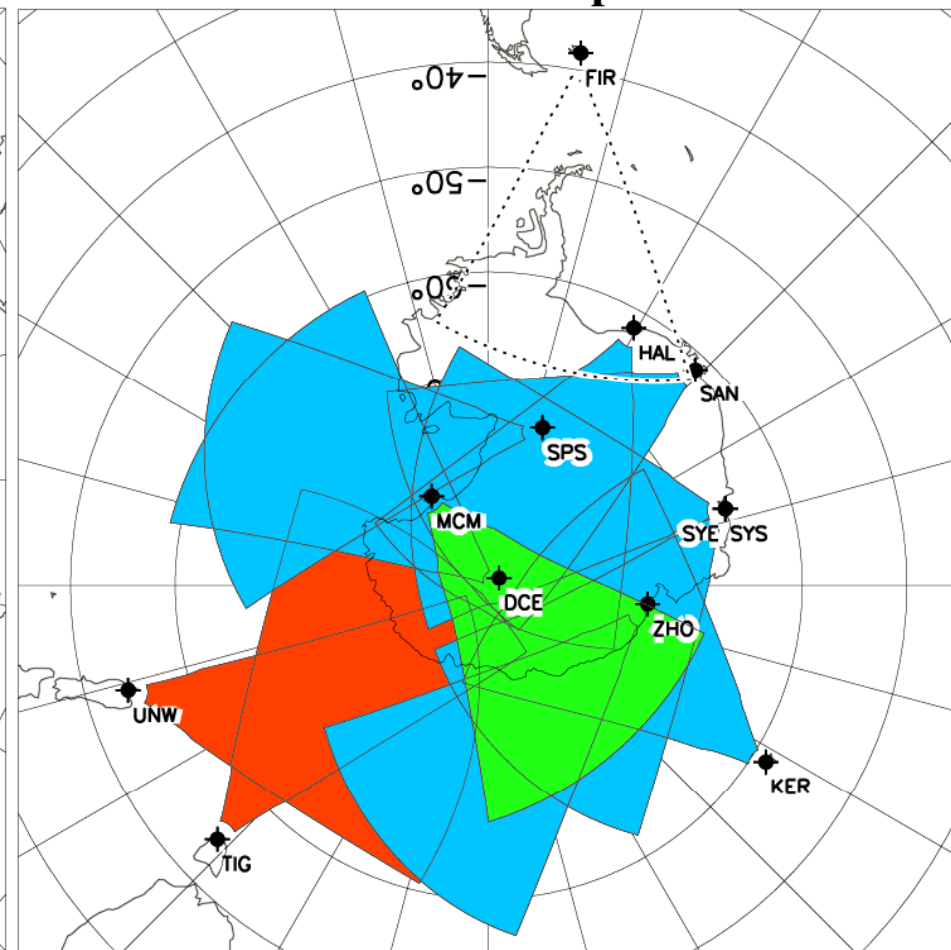
- In 1983 a single HF radar was built at Goose Bay, Labrador by a group from JHU/APL led by Ray Greenwald
- The aim was to demonstrate the viability of using coherent backscatter from the auroral F region to study the ionosphere, magnetosphere, and coupling to the solar wind
- Followed by collaborative radar builds with French scientists at Schefferville, Quebec and U.K. scientists at Halley Bay, Antarctica (1980s)
- In the early 1990's discussions led to the founding of the international SuperDARN collaboration (U.S., U.K., Canada, France, Japan, South Africa)
- Now SuperDARN operates about 35 radars and involves the funding agencies of ~10 countries

SuperDARN Radar Coverage – January 1, 2013

Northern Hemisphere



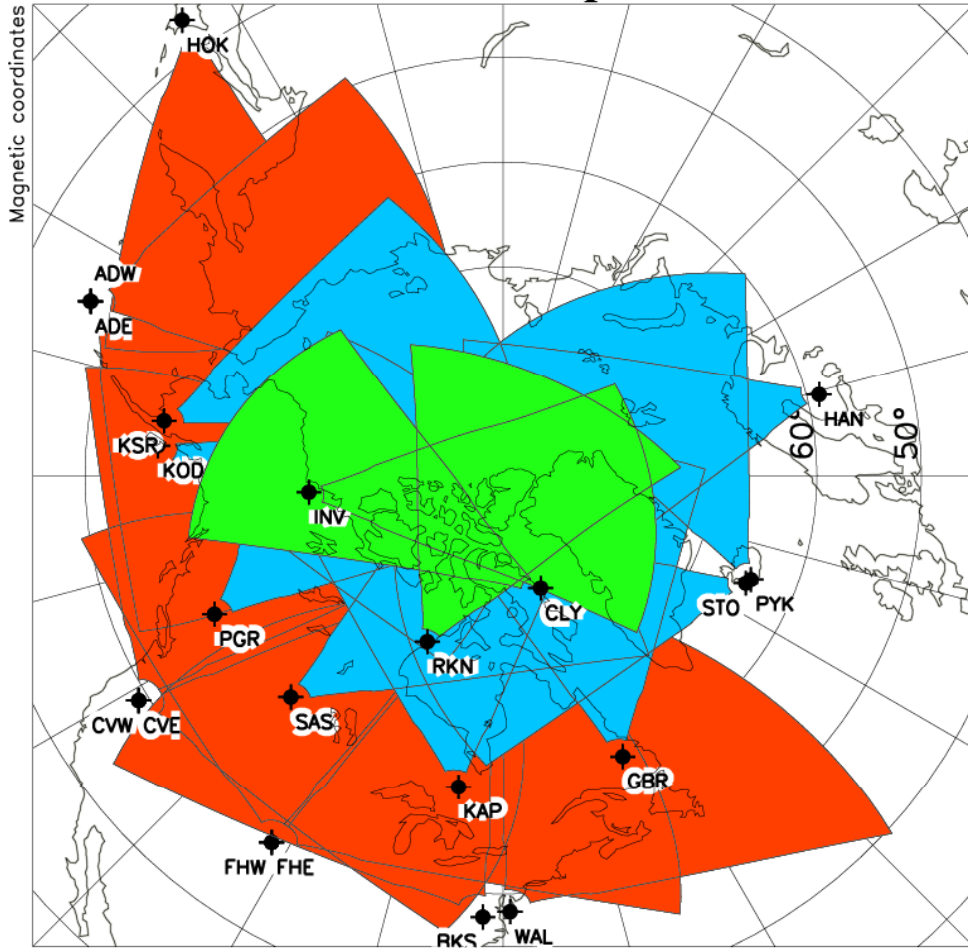
Southern Hemisphere



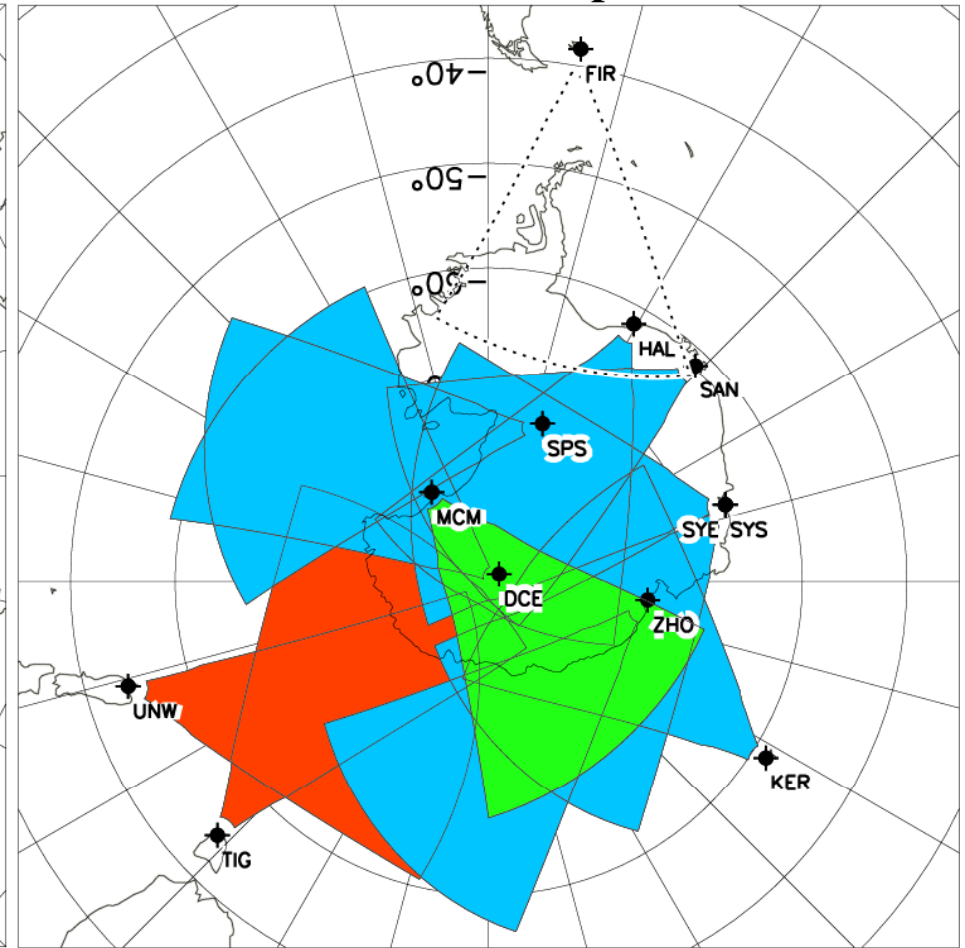
■ Polar Cap ■ High-Latitude ■ Mid-Latitude Out-of-Service

SuperDARN Radar Coverage – January 1, 2013

Northern Hemisphere



Southern Hemisphere



■ Polar Cap ■ High-Latitude ■ Mid-Latitude Out-of-Service

Coverage in the Russian sector has now begun with the completion of the Ekaterinburg radar (ISTP SB RAS)

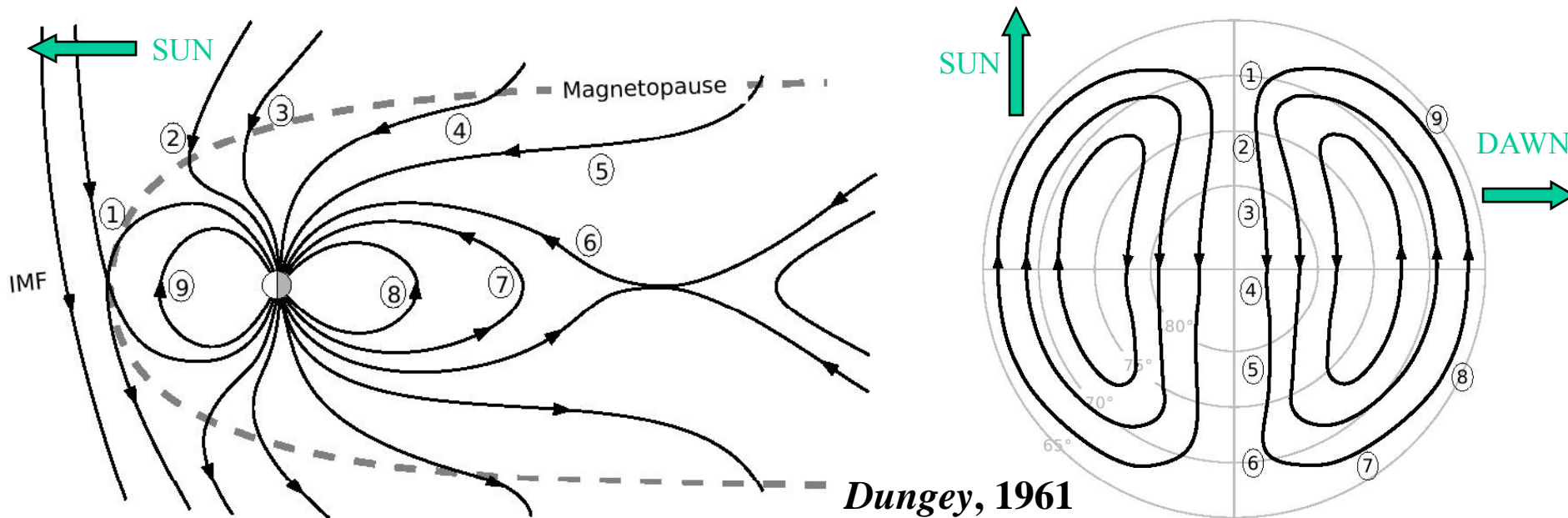
SuperDARN: A funny name

- Stands for: Super Dual Auroral Radar Network
- The radars are oriented in pairs, hence dual, and the network is super because it covers both the northern and southern hemispheres
- The original network of radars was built to cover auroral latitudes
- SuperDARN is a large international collaboration with ~15 Principal Investigator (PI) groups
- The radars operate on a common schedule and the data are freely shared between the PI groups
- Over the last ten years, coverage has expanded with the construction of networks that cover the polar cap and mid-latitudes

SuperDARN: Brief facts

- The radars are relatively inexpensive and operate automatically and all the time
- Radar scan time is usually 1 or 2 minutes
- The radar monitor the weather in Earth's near-space environment, including the effects of large geomagnetic storms that are due to solar flares
- The best-known SuperDARN product to the research community are time-varying maps of the large-scale pattern of plasma convection

Concept of Ionospheric Plasma Convection

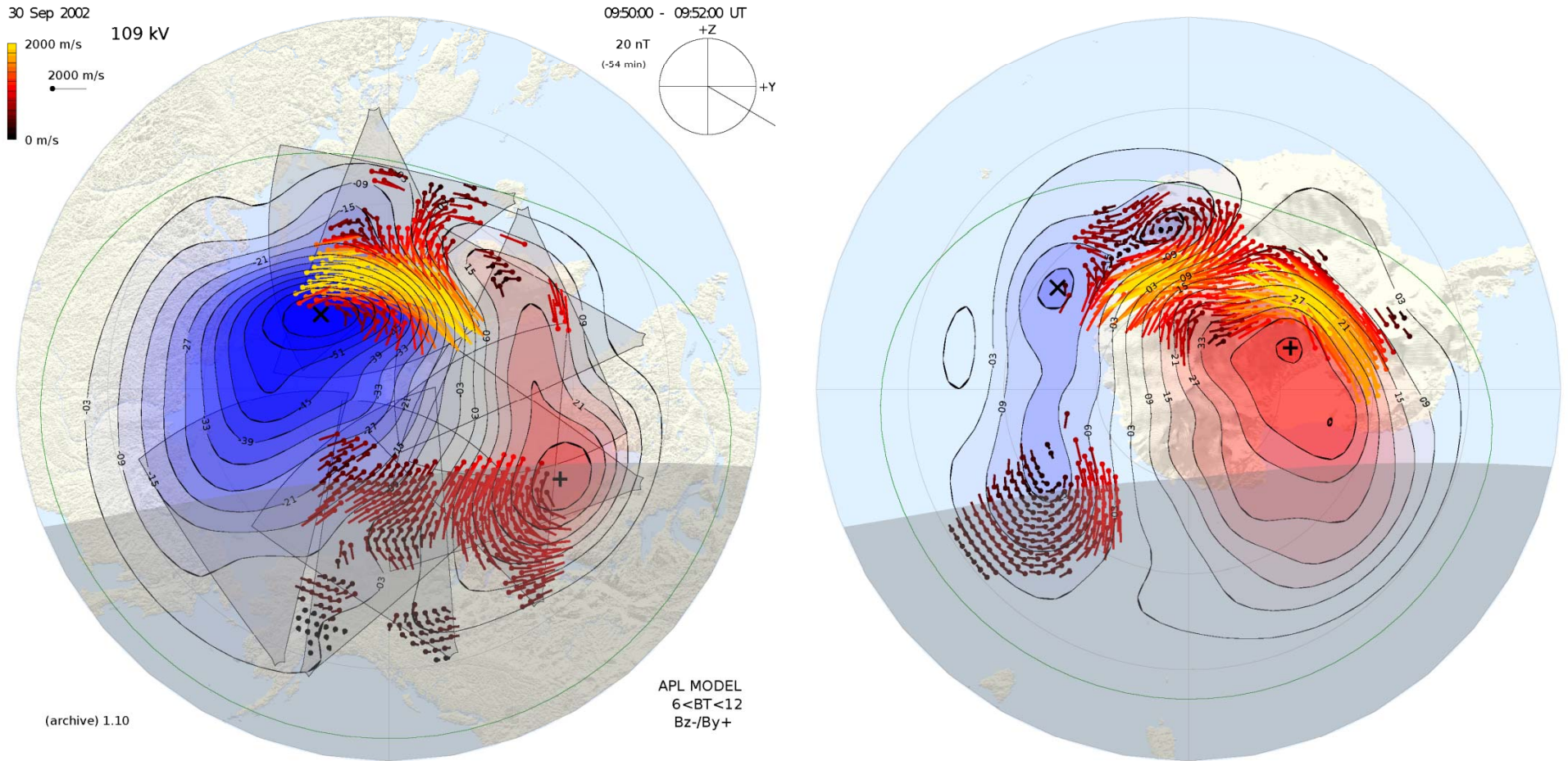


- The outer magnetosphere and high latitude ionosphere are coupled via electric fields and currents that are transmitted along quasi-equipotential magnetic field lines.
- Plasma convection in the magnetosphere driven by the solar wind and interplanetary magnetic field (IMF) is mirrored in the ionospheric convection at high latitudes.
- Measurements of convection velocity from the SuperDARN radars can be combined (assimilated) into maps of the global convection pattern.

Global-Scale Mapping of Ionospheric Plasma Convection

Assimilation of observational and model data into maps [Ruohoniemi and Baker, 1998]

September 30, 2002: 09:50 – 09:52 UT

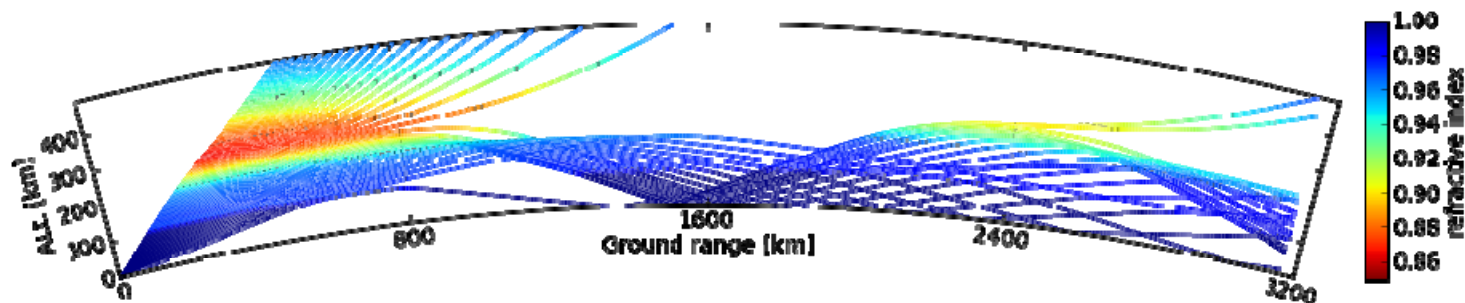


Northern Hemisphere

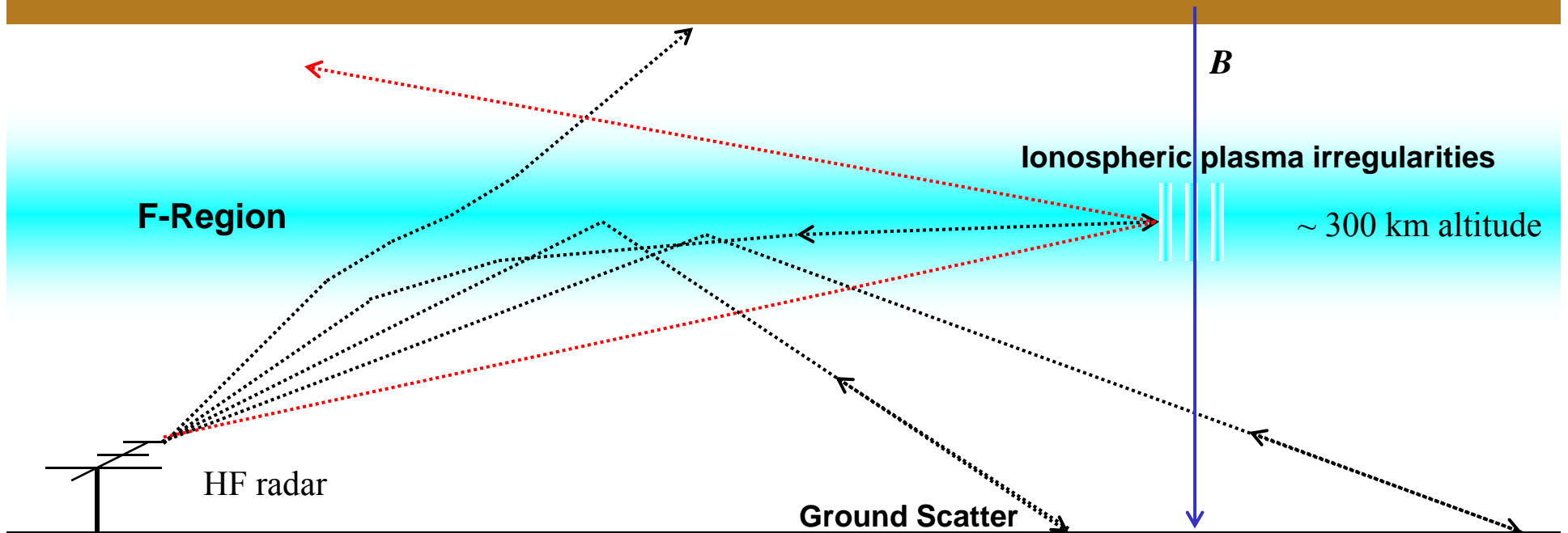
Southern Hemisphere

Part II Primer on HF Radar and Coherent Backscattering

- High Frequency (HF) radars operate at ~ 10 MHz (wavelengths of tens of meters)
- An early success of HF radar (1930s) was the first direct measurement of the properties of the ionosphere
- HF rays are bent, or refracted, by the ionosphere and can propagate to great distances leading to:
 - Short wave radio propagation
 - Over-The-Horizon (OTH) radar



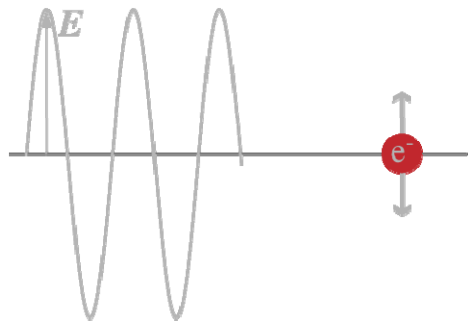
Propagation and Scattering of HF Signal



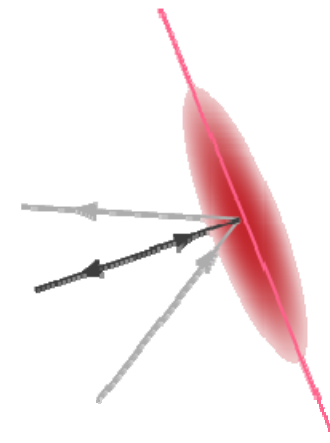
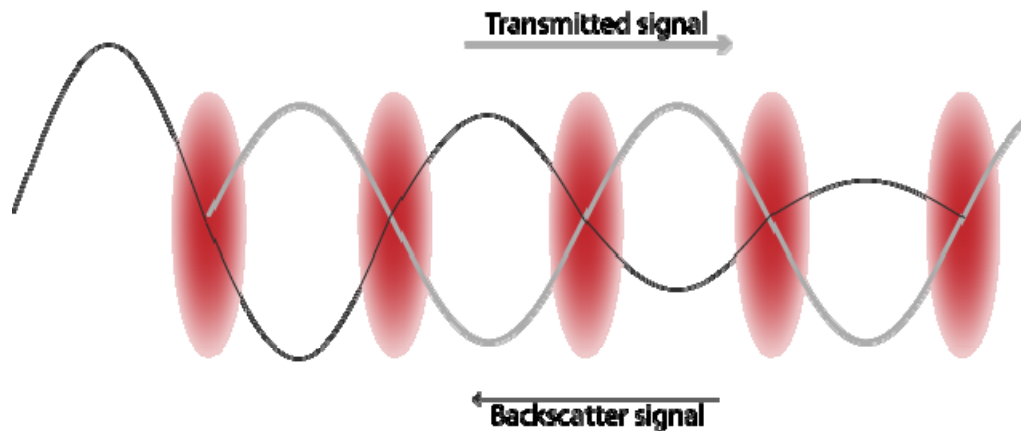
- HF rays are refracted in the ionosphere as they encounter gradients in electron density.
- Transmitted signals can be reflected back to the radar by:
 - 1) Ionospheric plasma irregularities (Field-Aligned Irregularities, or FAIs)
 - 2) Earth's surface ('ground scatter')
- Information about the reflectors is carried in the returned signal, e.g., Doppler velocity

Coherent Scattering from Ionospheric Irregularities

- Conditions required to observe ionospheric scatter with SuperDARN radars



EM backscatter generated by free electrons in the ionosphere accelerated by a transmitted signal.



Backscatter is amplified under Bragg conditions by density fluctuations with scale sizes on the order of half the transmitted wavelength.

Orthogonality of the transmitted signal with the background magnetic field (aspect condition) guarantees maximum returned power.

HF Radar Backscatter from Ionospheric Irregularities

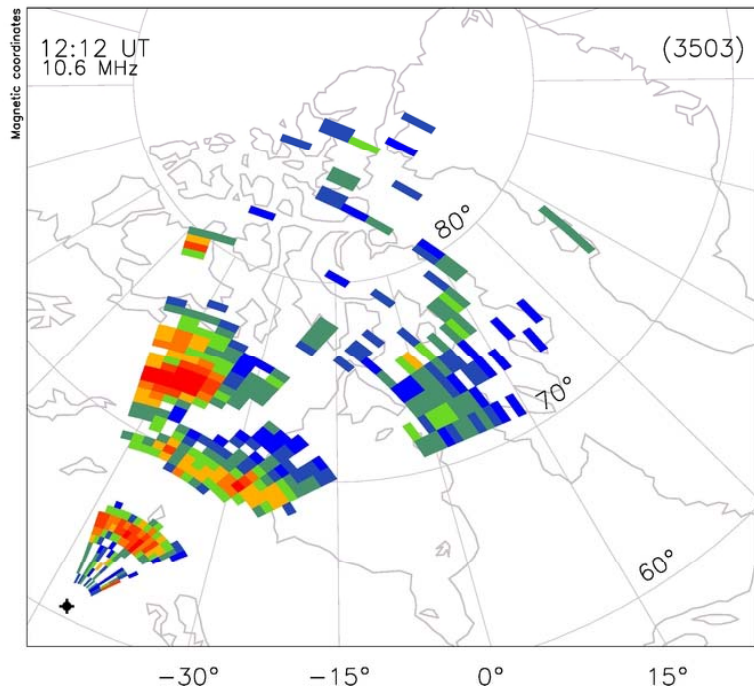
Observations with the Saskatoon radar: December 19, 2013 12:12-12:13 UT

Saskatoon (fitACF) Ch A
default g-s flag

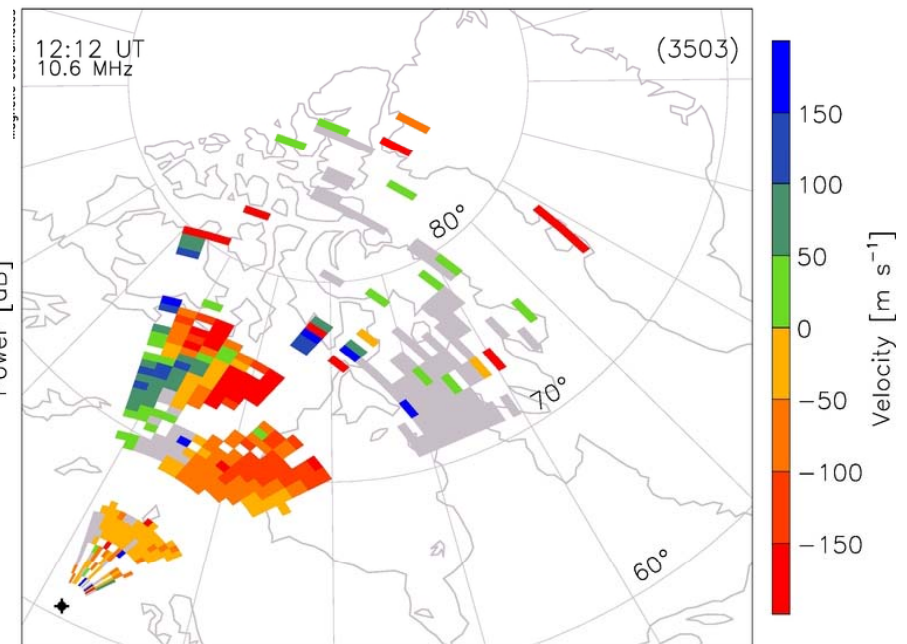
19/Dec/2013 12:12:00.0
to
19/Dec/2013 12:12:00.0

Saskatoon (fitACF) Ch A
default g-s flag

19/Dec/2013 12:12:00.0
to
19/Dec/2013 12:12:00.0



Backscattered power (dB)



Line-of-sight velocity (m/s)

The observation of coherent backscatter from FAIs depends on (i) the presence of irregularities and (ii) propagation at favorable magnetic aspect angle

HF Radar Backscatter from Ionospheric Irregularities

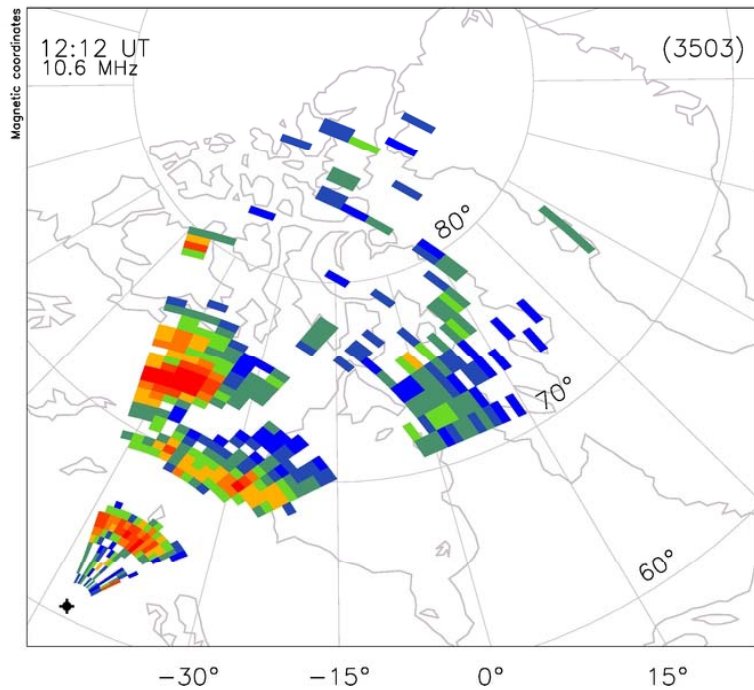
Observations with the Saskatoon radar: December 19, 2013 12:12-12:13 UT

Saskatoon (fitACF) Ch A
default g-s flag

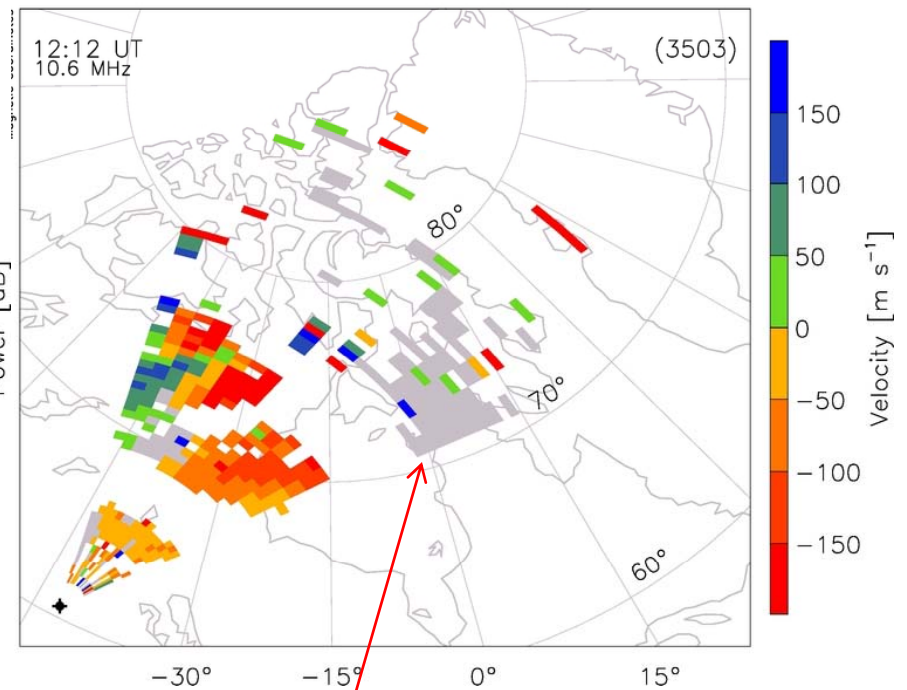
19/Dec/2013 12:12:00.0
to
19/Dec/2013 12:12:00.0

Saskatoon (fitACF) Ch A
default g-s flag

19/Dec/2013 12:12:00.0
to
19/Dec/2013 12:12:00.0



Backscattered power (dB)

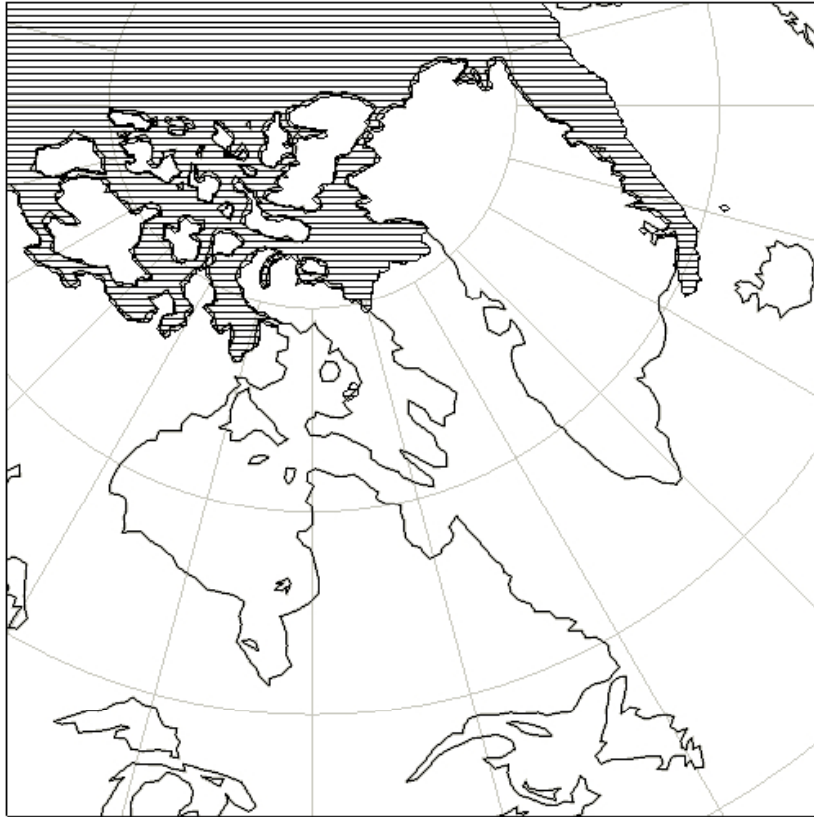


Line-of-sight velocity (m/s)

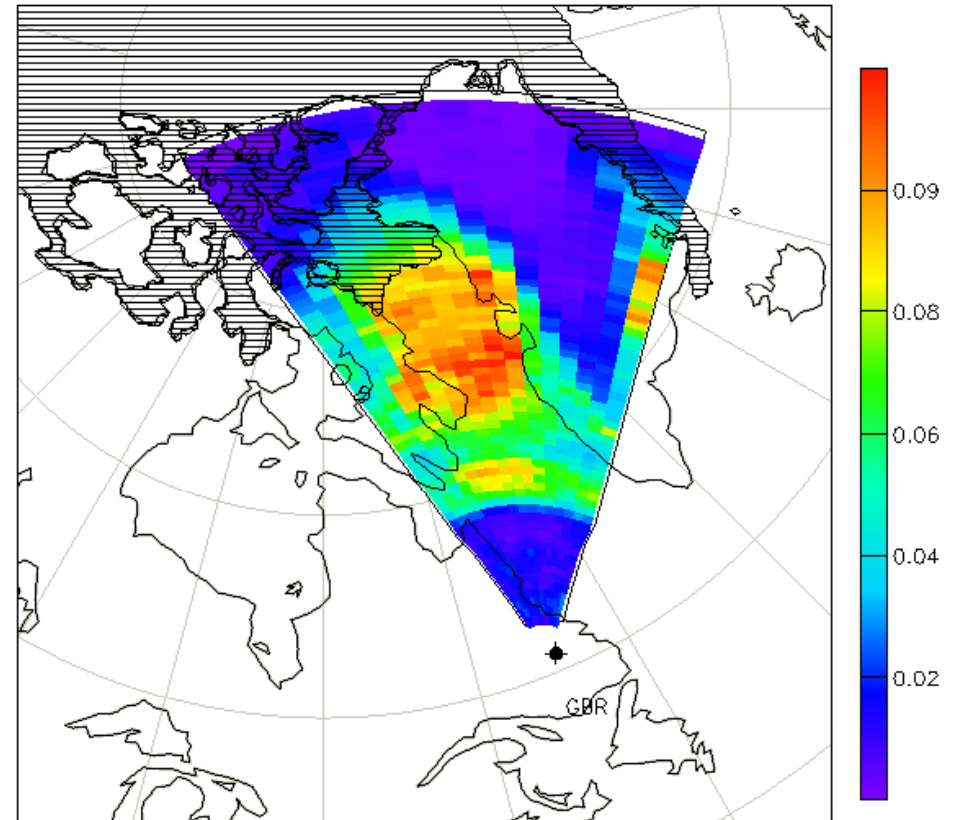
Grey scale indicates ground scatter

HF Radar Backscatter from Earth's Surface

Student project: Comparison of sea ice cover and distribution of ground scatter



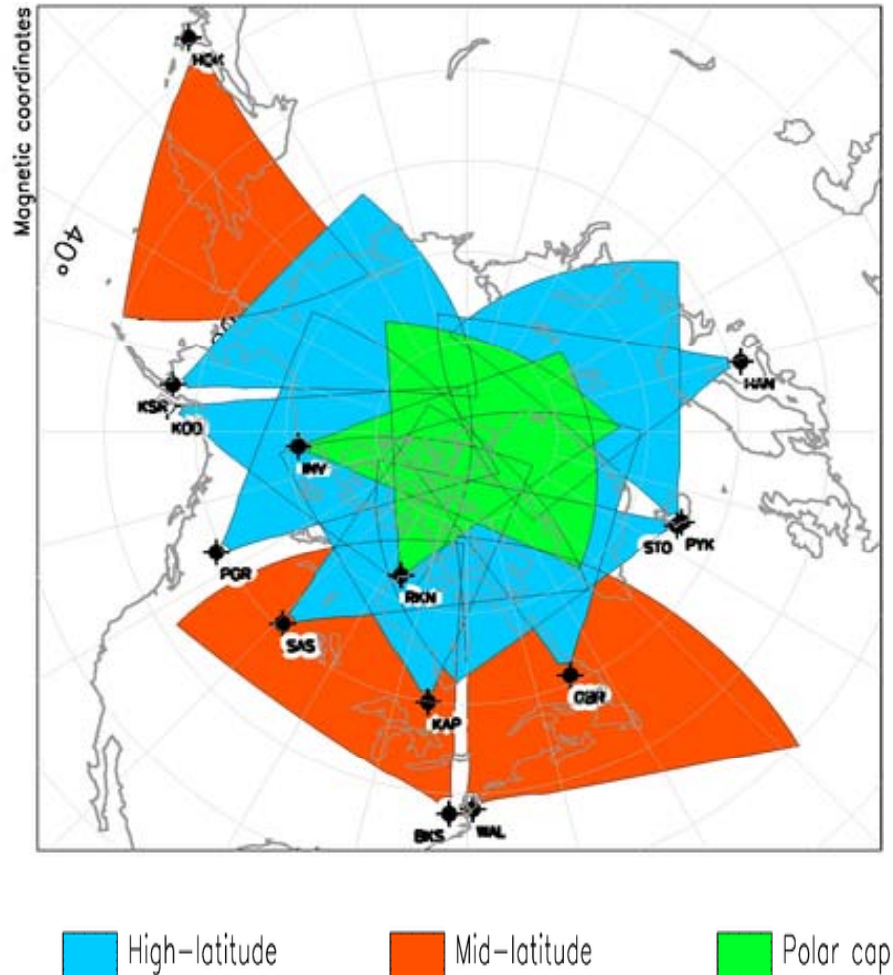
- Furthest extent of sea ice cover during month of October 2000 (National Snow and Ice Data Center, Boulder, CO).



- Ground scatter occurrence rate observed by the radar at Goose Bay during daytime over the month of October 2000.

Part III Expansion of SuperDARN to Mid-Latitudes

January 1, 2009



First mid-latitude SuperDARN radars were built in the mid-2000s at Wallops , (Virginia), Hokkaido (Japan), and Blackstone (Virginia)

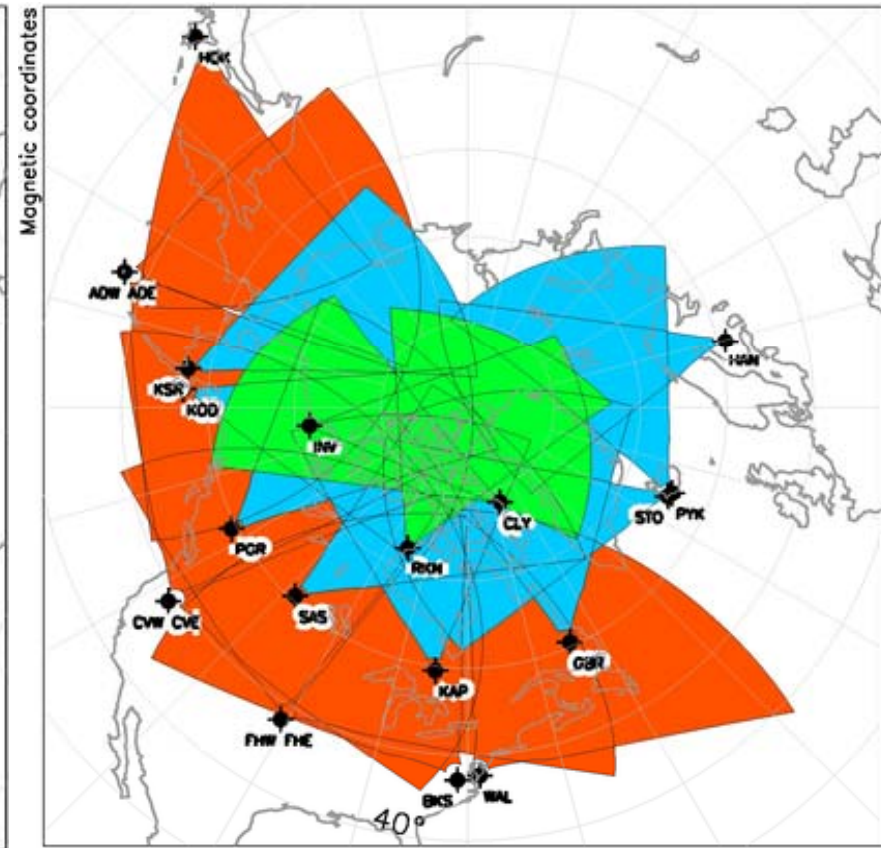
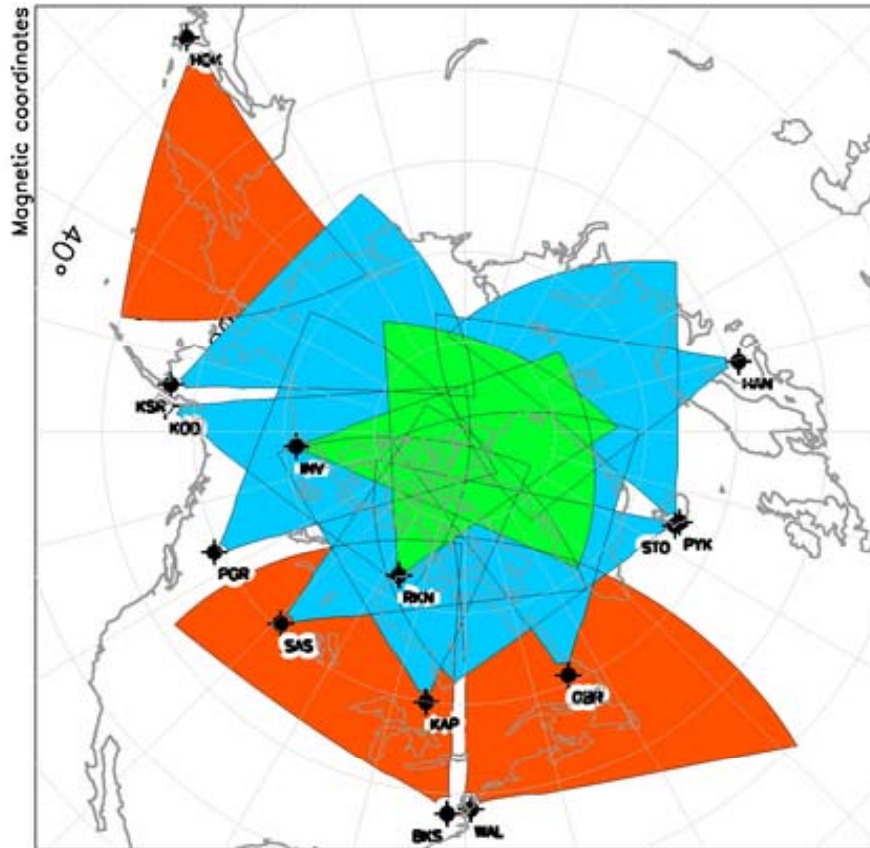
The construction of a mid-latitude chain of SuperDARN radars began in 2009 funded by the U.S. National Science Foundation (NSF) Mid-Sized Infrastructure (MSI) program

The MSI build is a collaboration between the four U.S. SuperDARN universities

Expansion of SuperDARN to Mid-Latitudes

January 1, 2009

January 1, 2013



High-latitude

Mid-latitude

Polar cap

2009 - Hays, Kansas

2010 - Christmas Valley, Oregon

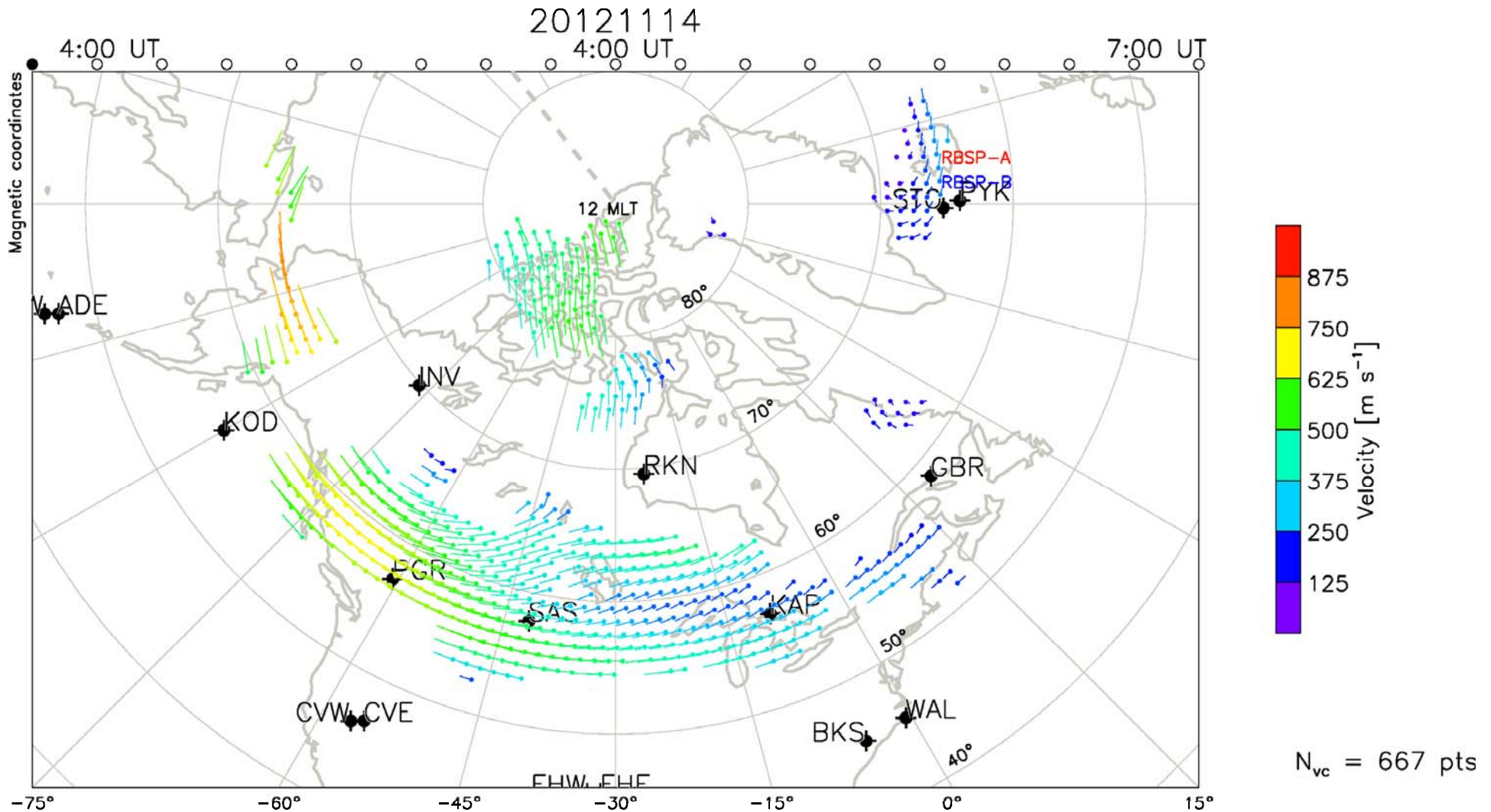
2012 - Adak, Alaska

Two-radar SuperDARN site at Fort Hays, Kansas



Aerial photo: one radar is oriented towards the NE, the other towards the NW

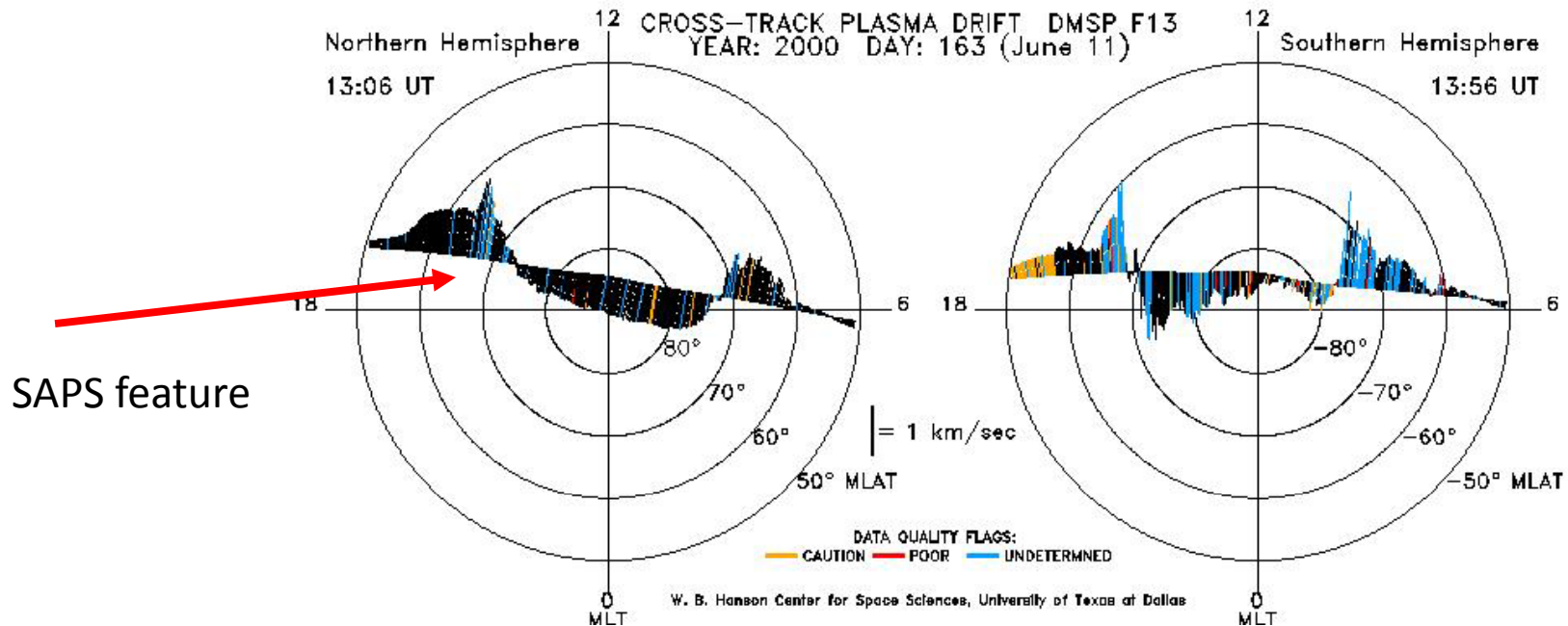
Expanded Observations of Plasma Convection during Storms



Fitted velocity vectors during storm: Nov. 14, 2012, 4 – 7 UT

New Capabilities: Mid-Latitude SuperDARN Radars

- With mid-latitude radars we can image the expanded pattern of convection during geomagnetic storms
- This includes large-scale mapping of the sub-auroral polarization stream (SAPS) first reported by Galperin et al. [1986] as the Polar Jet
- Previously only viewed in single cuts from satellite passes such as DMSP

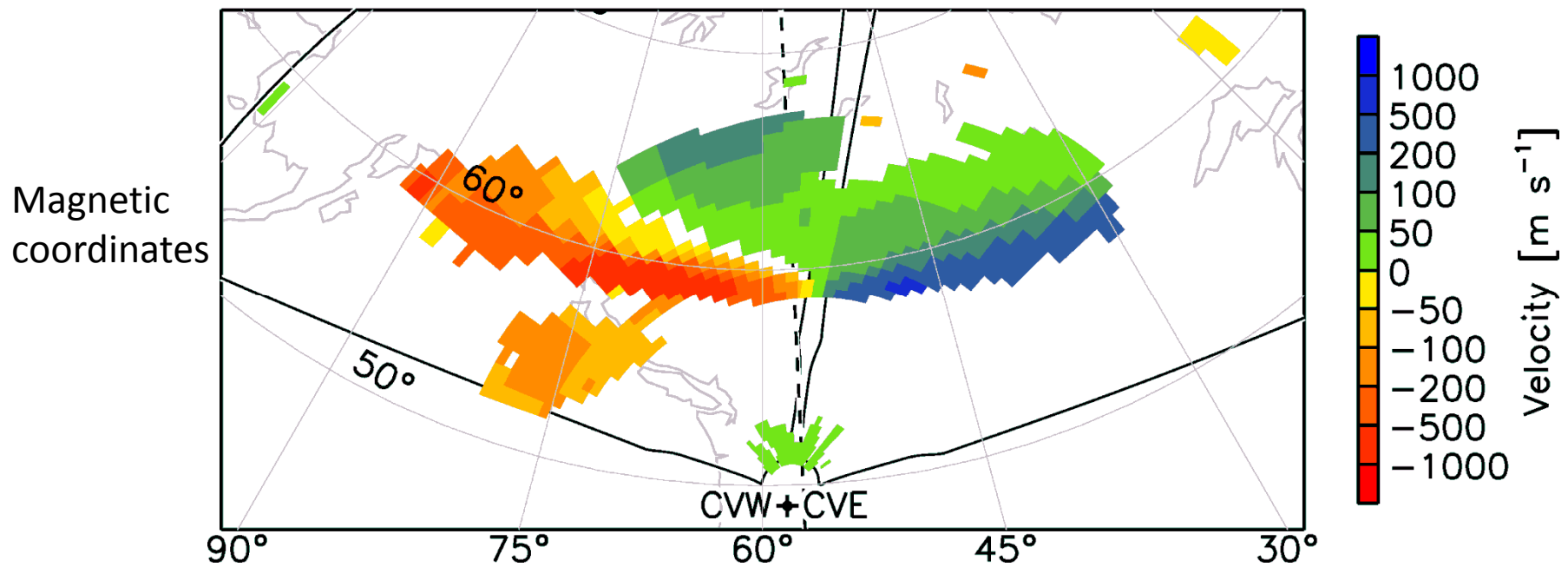


SAPS Observations – April 9, 2011

Line-of-sight velocity measurements

O840 UT

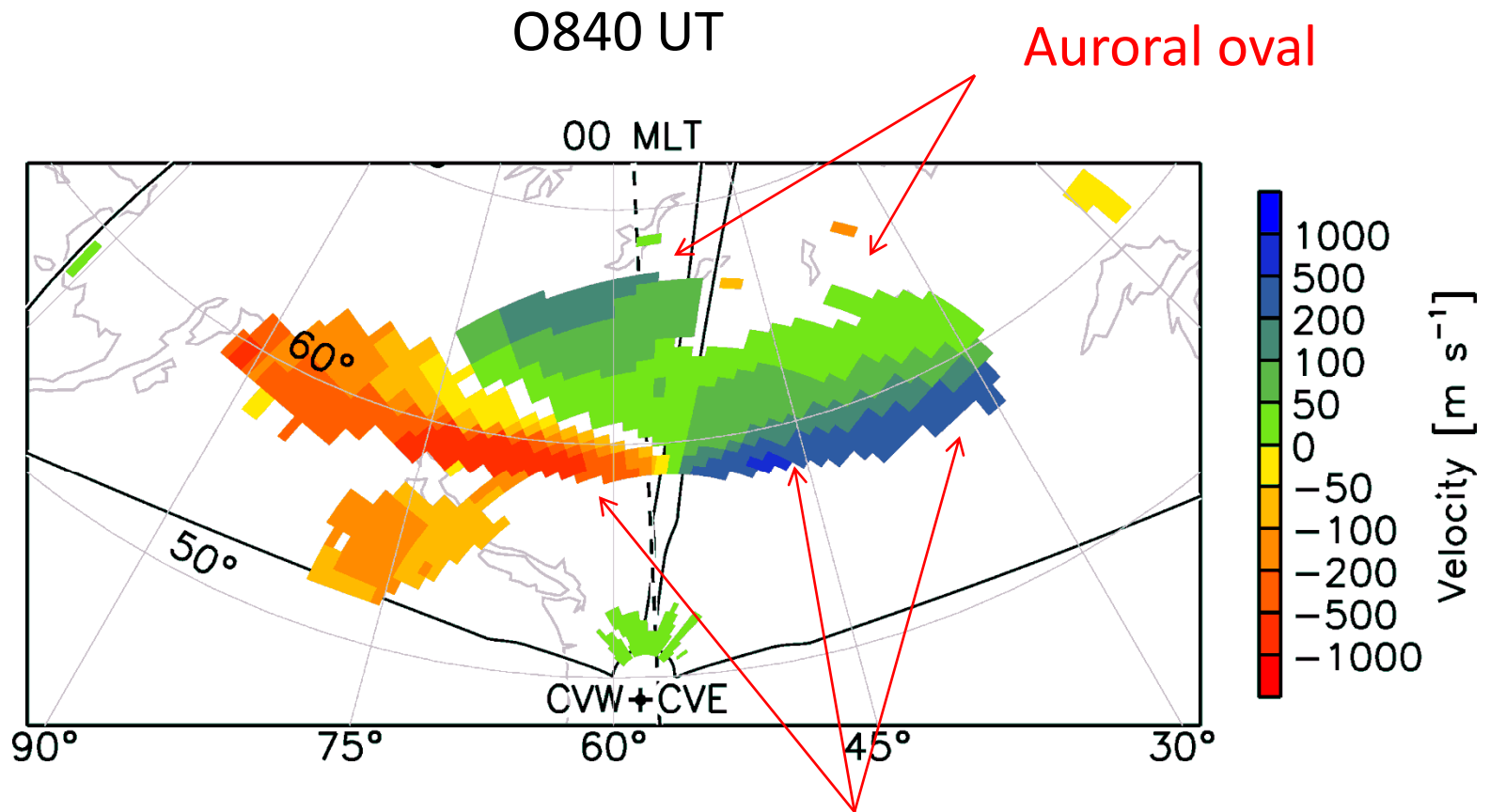
00 MLT



Fields of view of the Christmas Valley West and East radars (Oregon)

SAPS Observations – April 9, 2011

Line-of-sight velocity measurements

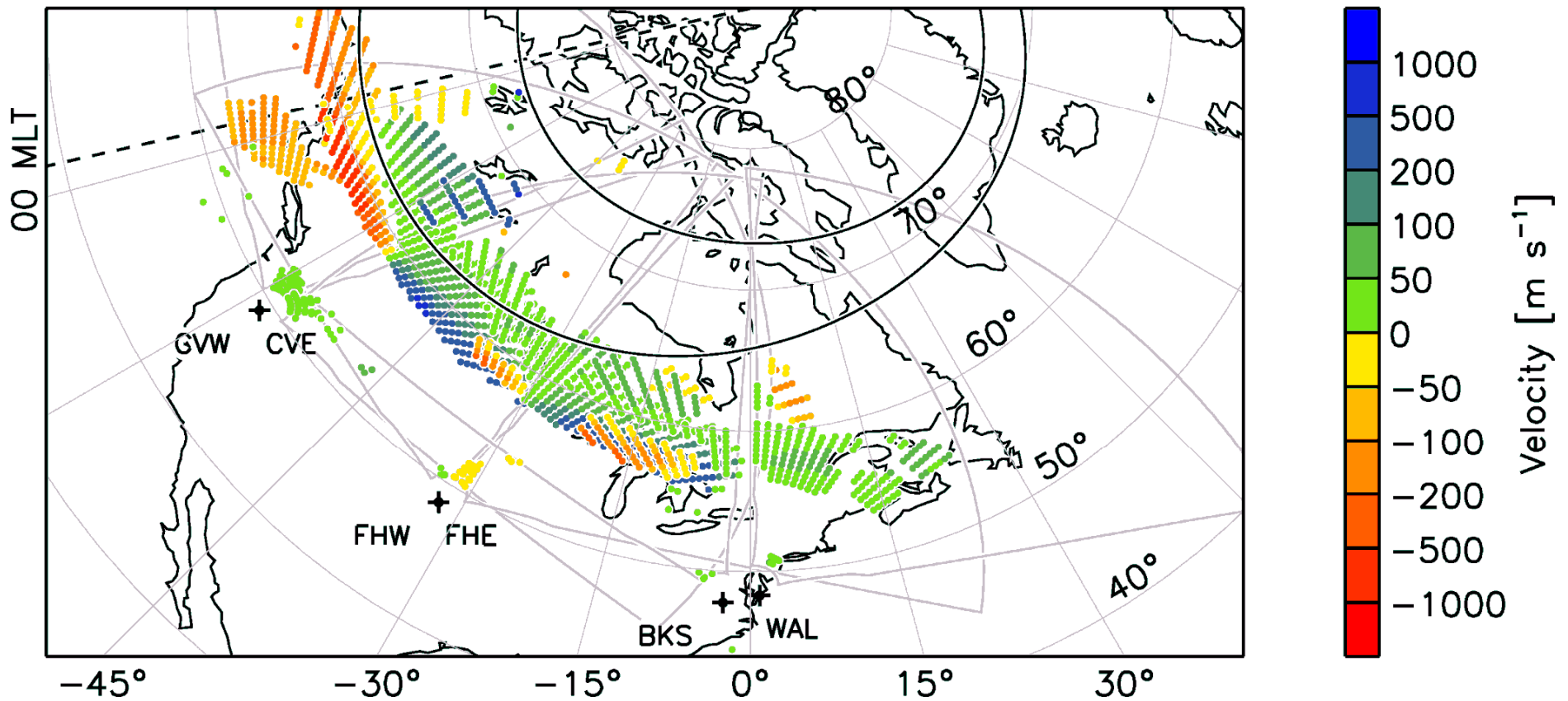


SAPS channel (Oksavik et al. [2006])

Large-Scale Map of SAPS Observations – April 9, 2011

0840 UT

[From Clausen *et al.*, 2012]

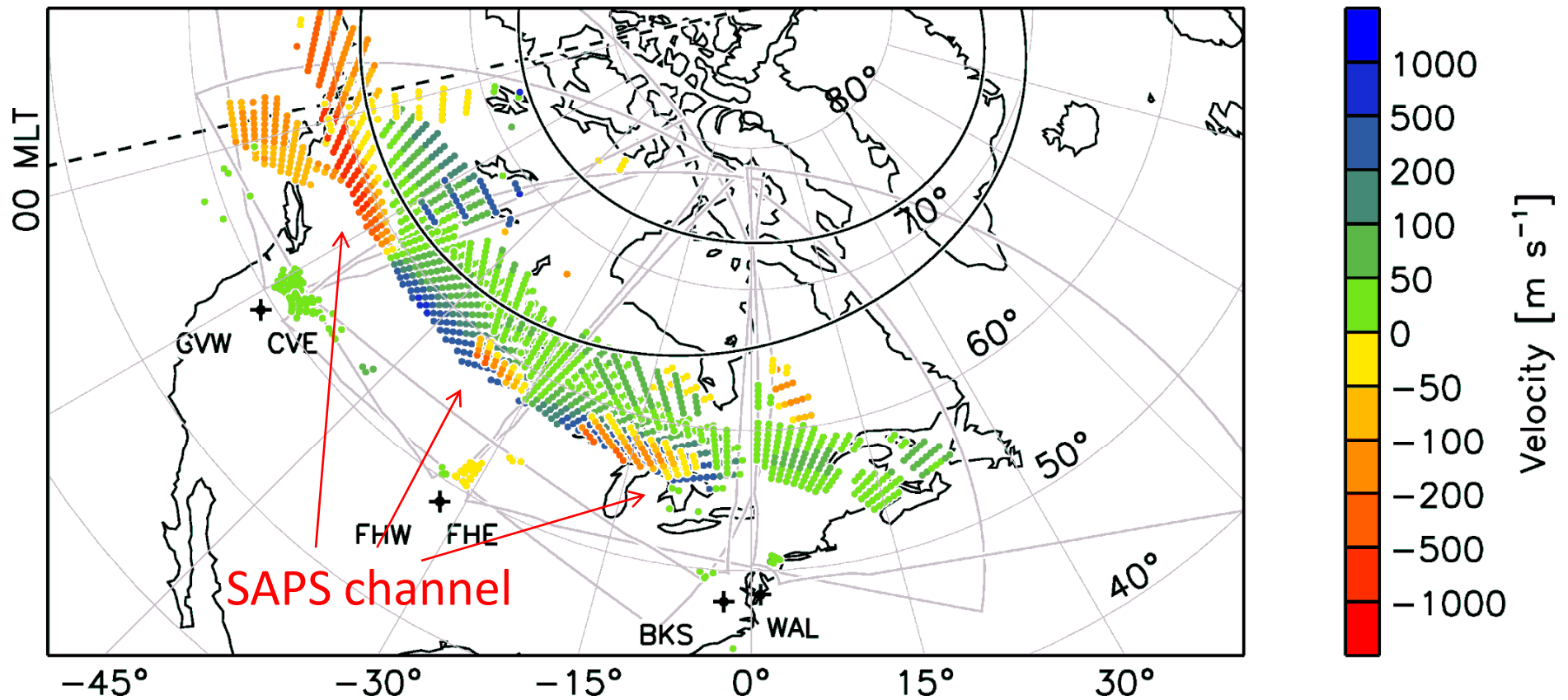


CVW/CVE – Christmas Valley E/W FHW/FHE – Fort Hays BKS/WAL – Blackstone/Wallops

Large-Scale Map of SAPS Observations – April 9, 2011

0840 UT

[From Clausen *et al.*, 2012]

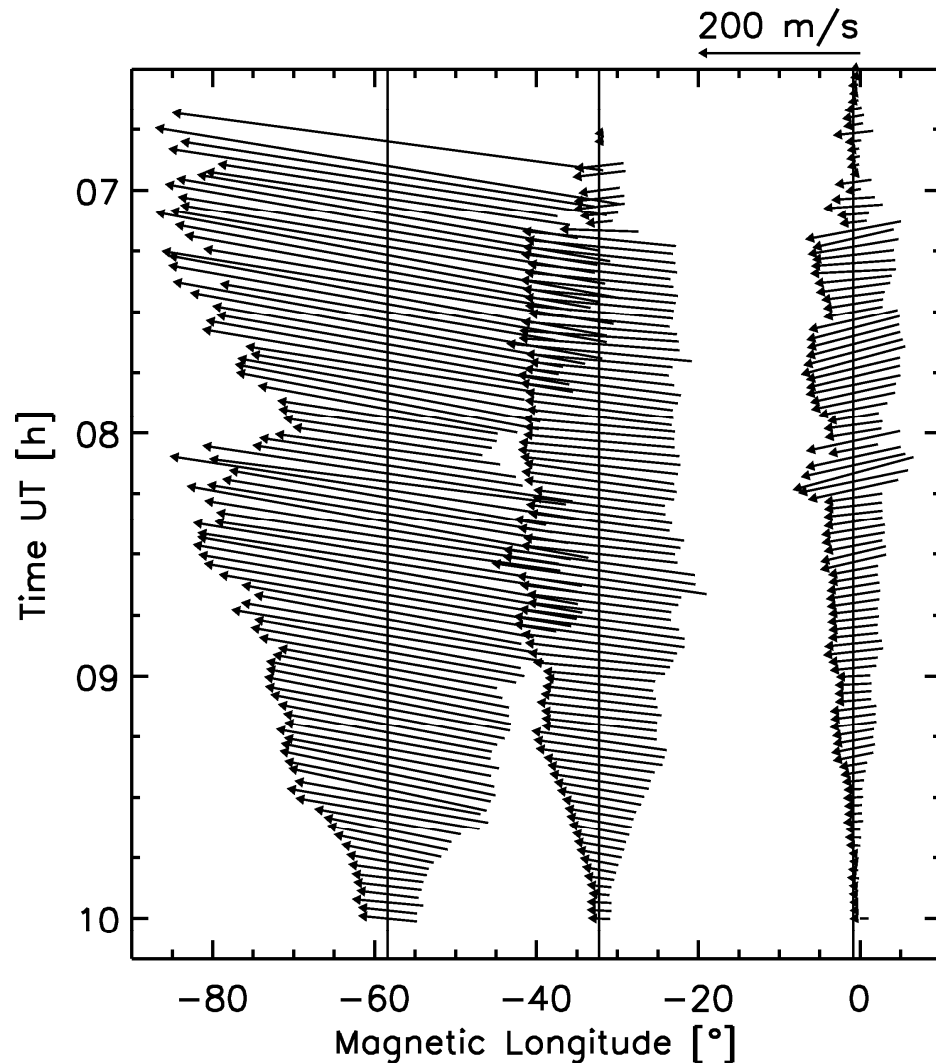


CVW/CVE – Christmas Valley E/W FHW/FHE – Fort Hays BKS/WAL – Blackstone/Wallops

April 9, 2011 - Inferred SAPS Velocities versus UT

Analysis of the peak velocities seen across pairs of radar observations produces estimates of SAPS velocity versus time and MLT

Observations of storm-time SAPS with SuperDARN span many hours of MLT for long periods of UT

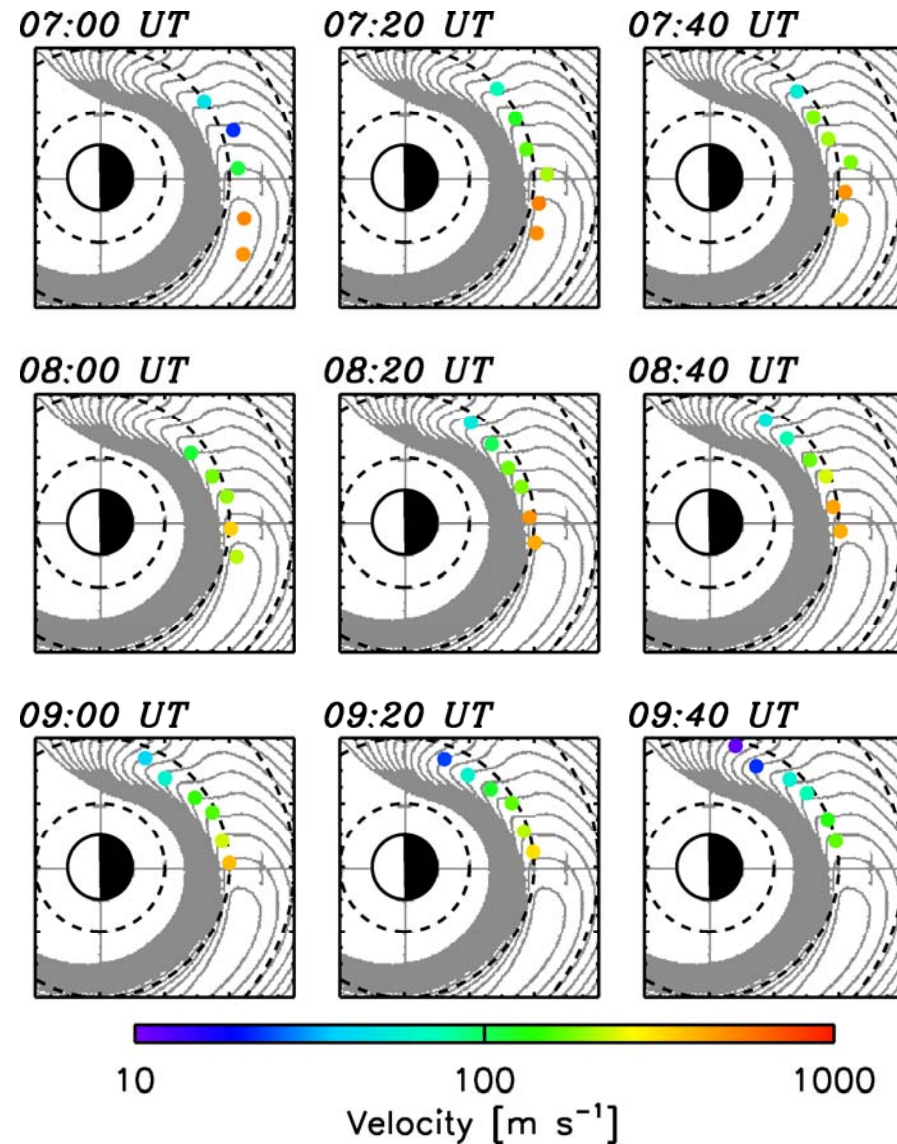


Projection of the SAPS into the Equatorial Plane

Locations of SAPS velocity maxima are mapped using T96 (colored dots).

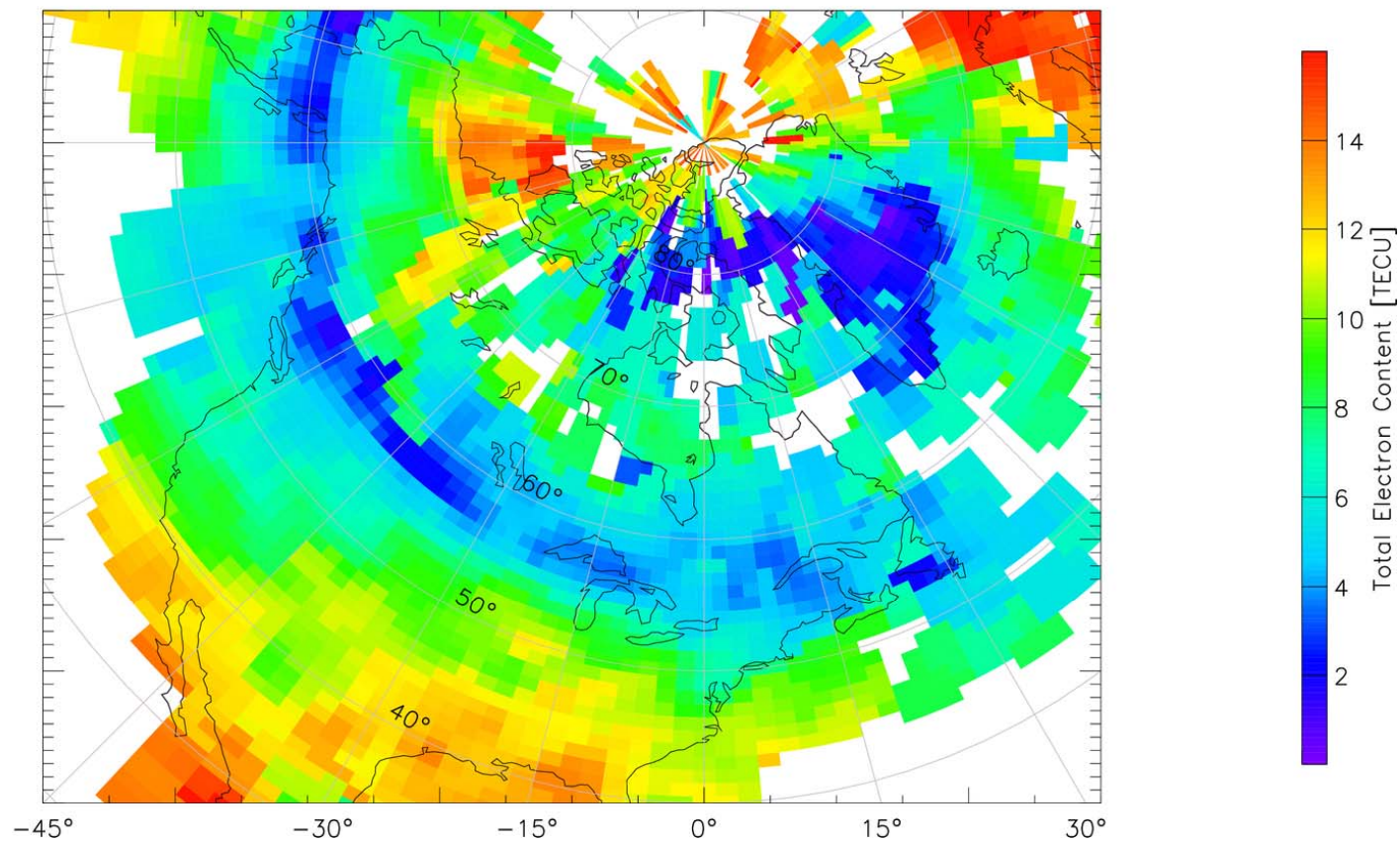
Contours of constant plasma pressure are taken from an RCM run for the same prevailing conditions.

Good correspondence indicates close coupling of the storm-time subauroral ionosphere with the inner magnetosphere



Mid-Latitude Disturbance: SAPS and TEC Trough

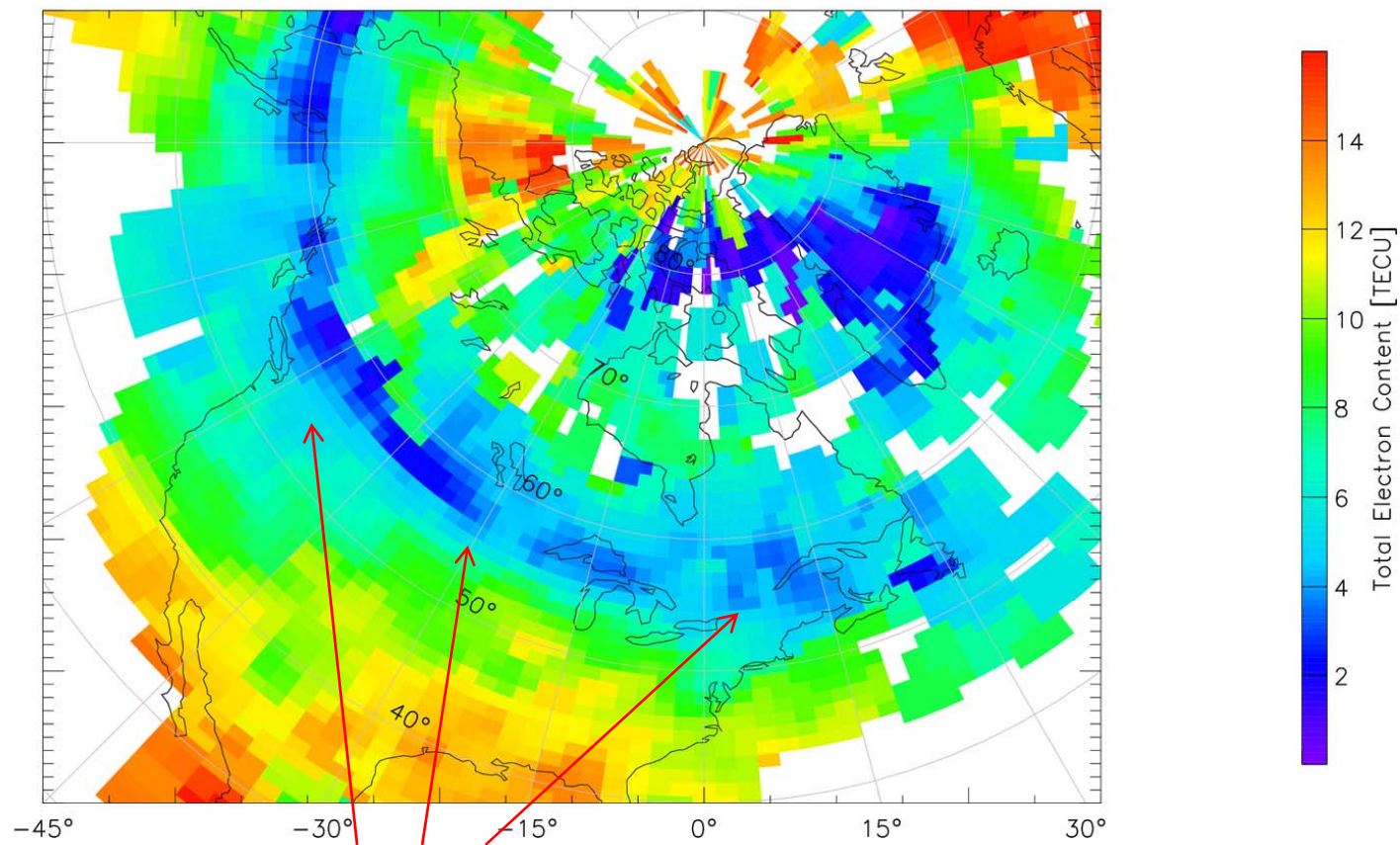
TOTAL ELECTRON CONTENT 09/Apr/2011 08:00:00.0
Median Filtered, Threshold = 0.01 to
09/Apr/2011 08:05:00.0



Map of the 'thickness' of the ionosphere measured by GPS satellites as the total count of electrons in a column of standard area

Mid-Latitude Disturbance: SAPS and TEC Trough

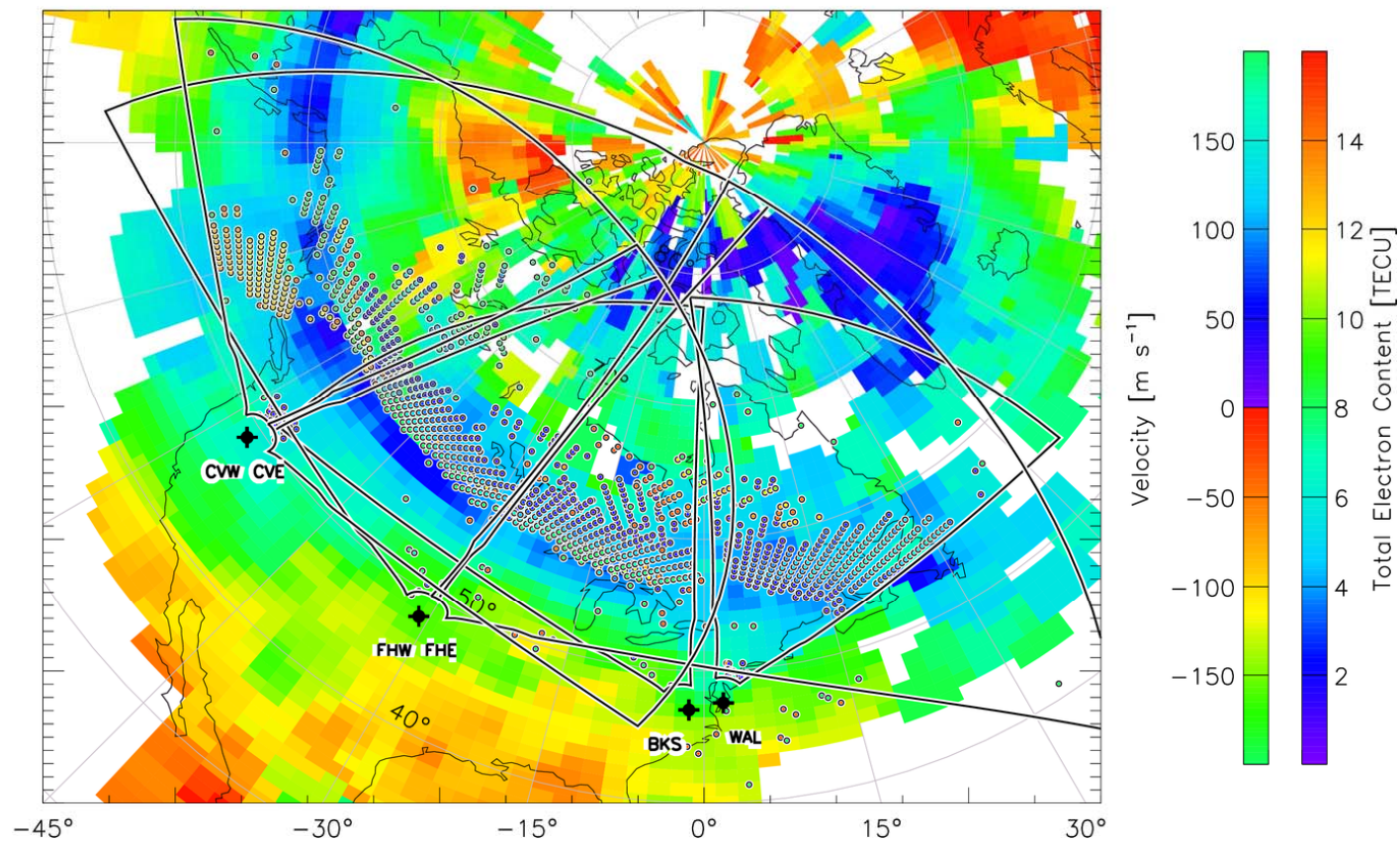
TOTAL ELECTRON CONTENT 09/Apr/2011 08:00:00.0
Median Filtered, Threshold = 0.01 to
09/Apr/2011 08:05:00.0



A mid-latitude 'trough' of very low plasma density as imaged in the TEC data across North America

Mid-Latitude Disturbance: SAPS and TEC Trough

TOTAL ELECTRON CONTENT 09/Apr/2011 08:00:00.0
Median Filtered, Threshold = 0.01 to
09/Apr/2011 08:05:00.0



Superimposed radar data show that the SAPS feature is associated with the TEC trough

SubAuroral Ionospheric Scatter - SAIS

- Shortly after the first mid-latitude radar came into operation at NASA Wallops Flight Facility in Virginia we observed a new kind of ionospheric backscatter
- It occurs throughout the night during geomagnetically quiet conditions
- Convection velocities are low (< 100 m/s)
- The ionospheric backscattering occurs at latitudes below the auroral zone, i.e., in the midlatitude region
- Described as SubAuroral Ionospheric Scatter (SAIS) by Ribeiro et al. [2012]

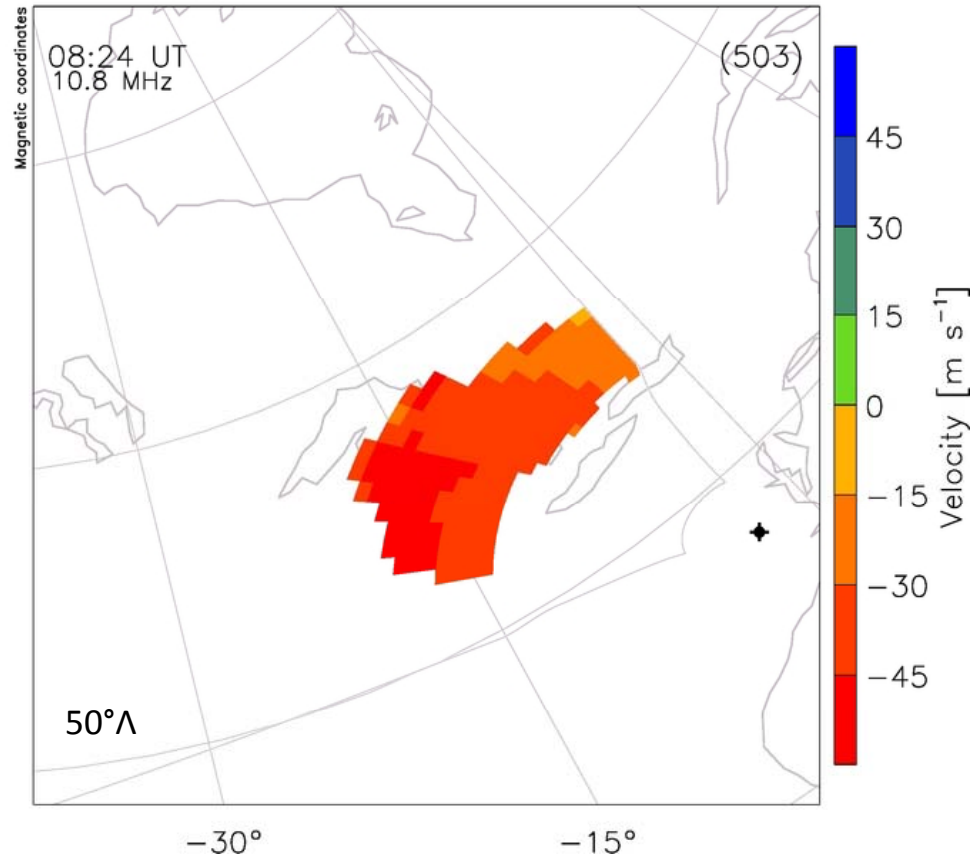
Example of a SAIS-derived Map of Subauroral Convection

Blackstone (fitACF) Ch A

05/Feb/2012 08:24:00.0
to
05/Feb/2012 08:24:00.0

Blackstone radar

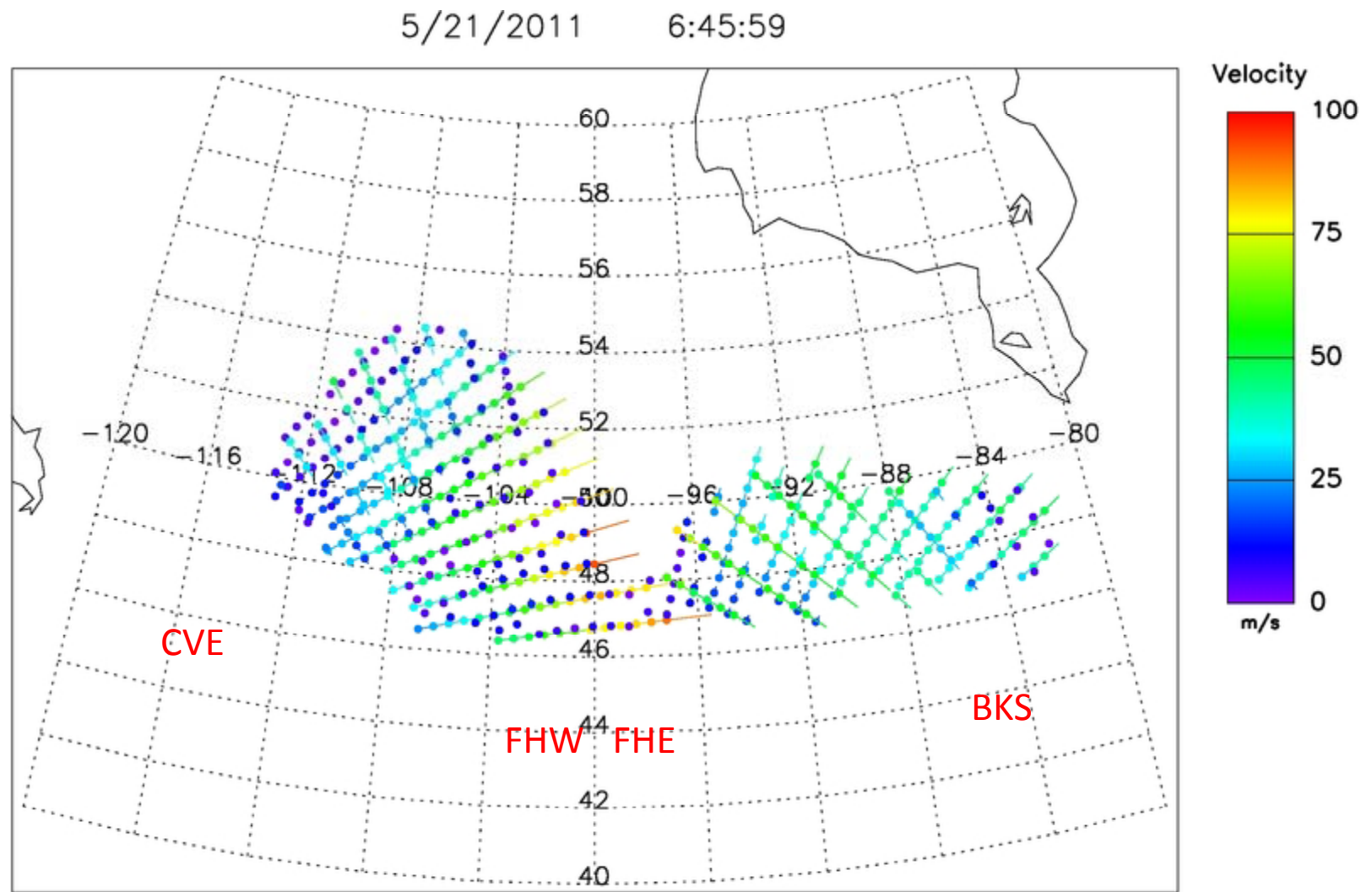
08:24 - 08:26 UT



Scan plot of SAIS showing variation in line-of-sight velocity with azimuth that is consistent with westward flow

Mapping Plasma Motion in the Mid-Latitude Ionosphere

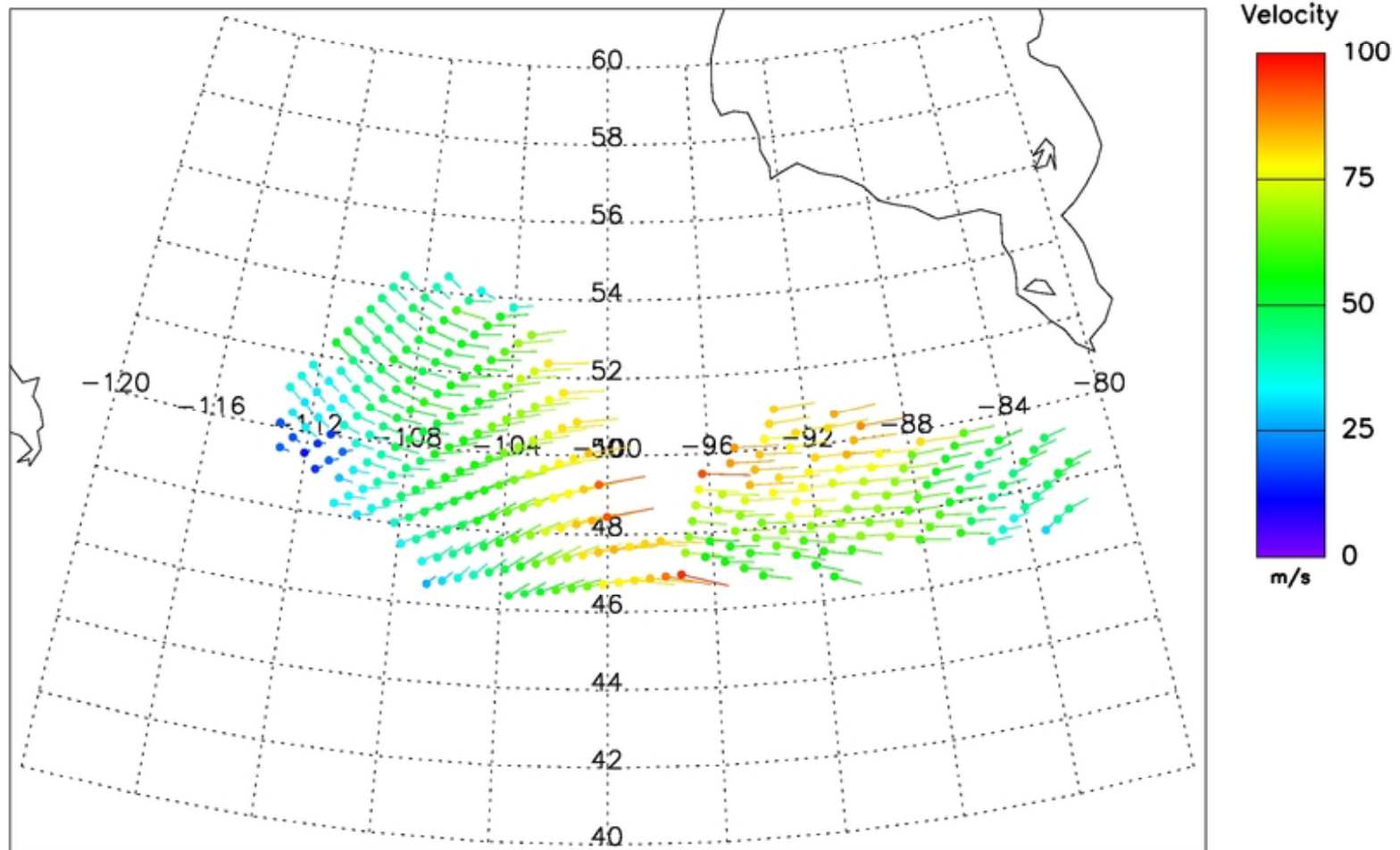
Common-volume LOS velocities measured by radars in Oregon, Kansas, and Virginia



Mapping Plasma Motion in the Mid-Latitude Ionosphere

Map of merged two-dimensional plasma velocity vectors

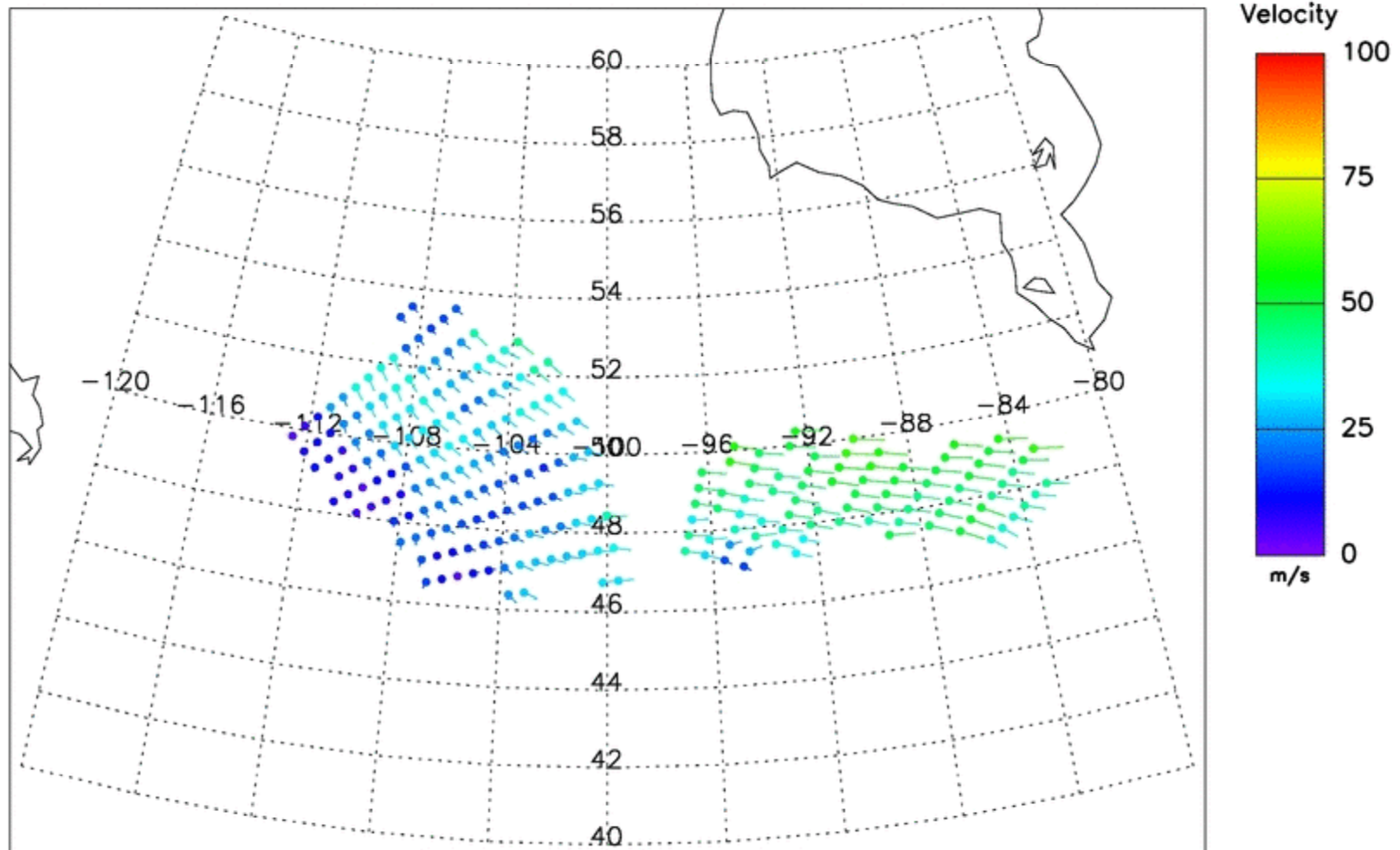
5/21/2011 6:45:59



Open question: Rapid Reversal in Mid-Latitude Plasma Convection

Twenty-minute movie showing a reversal in subauroral plasma velocity

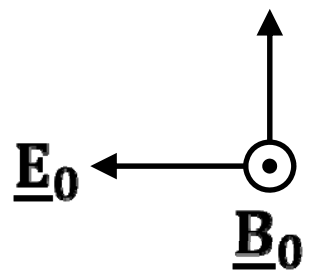
5/21/2011 6:40:0



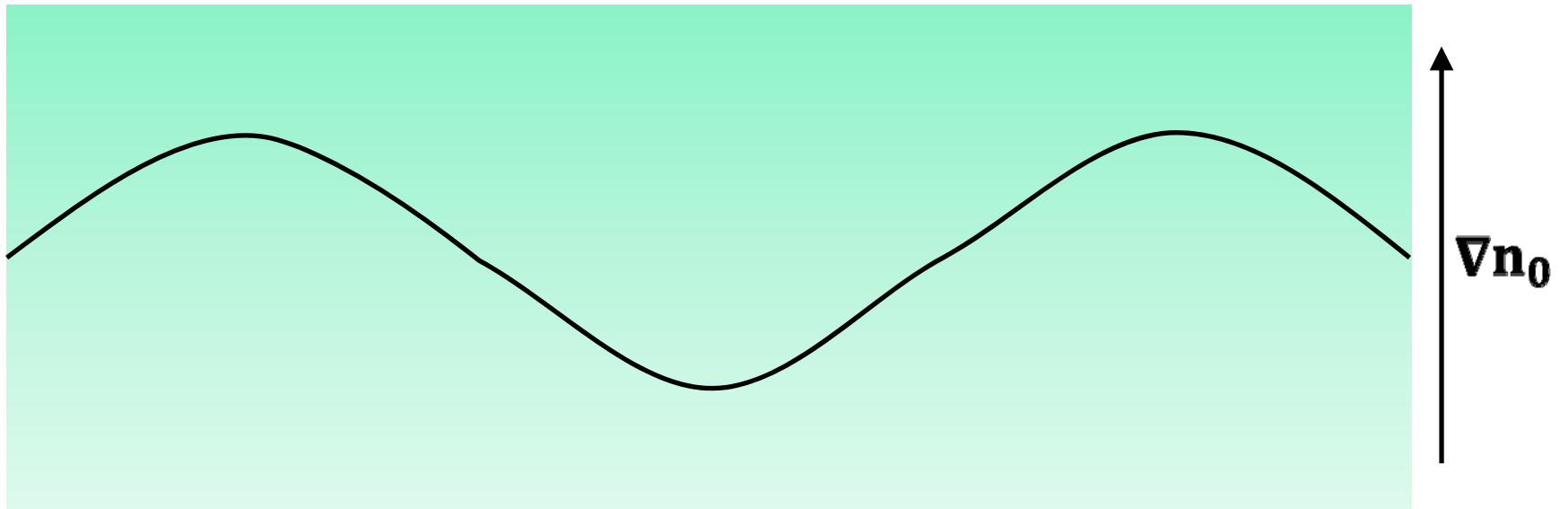
Part IV Ionospheric Plasma Instabilities

- The coherent scatter technique relies on the presence of irregularities in the plasma density with amplitudes ($\Delta N/N$) much larger than can be expected from thermal fluctuations
- These irregularities are due to plasma instabilities that amplify the thermal fluctuations
- Sources of free energy in the plasma include density and temperature gradients
- Not much is known about the instabilities responsible for the HF coherent backscatter!
- Irregularities could be generated at large scales (km) and then cascade down to the scales of the radar irregularities (tens of meters)

F region Gradient Drift Instability (GDI)

$$\underline{V}_0 = \underline{E}_0 \times \underline{B}_0$$


1. Consider an ambient background electric and magnetic field in a region with a horizontal density gradient parallel to the $\underline{E}_0 \times \underline{B}_0$ drift. Let the density be perturbed by a small-amplitude sinusoidal wave.

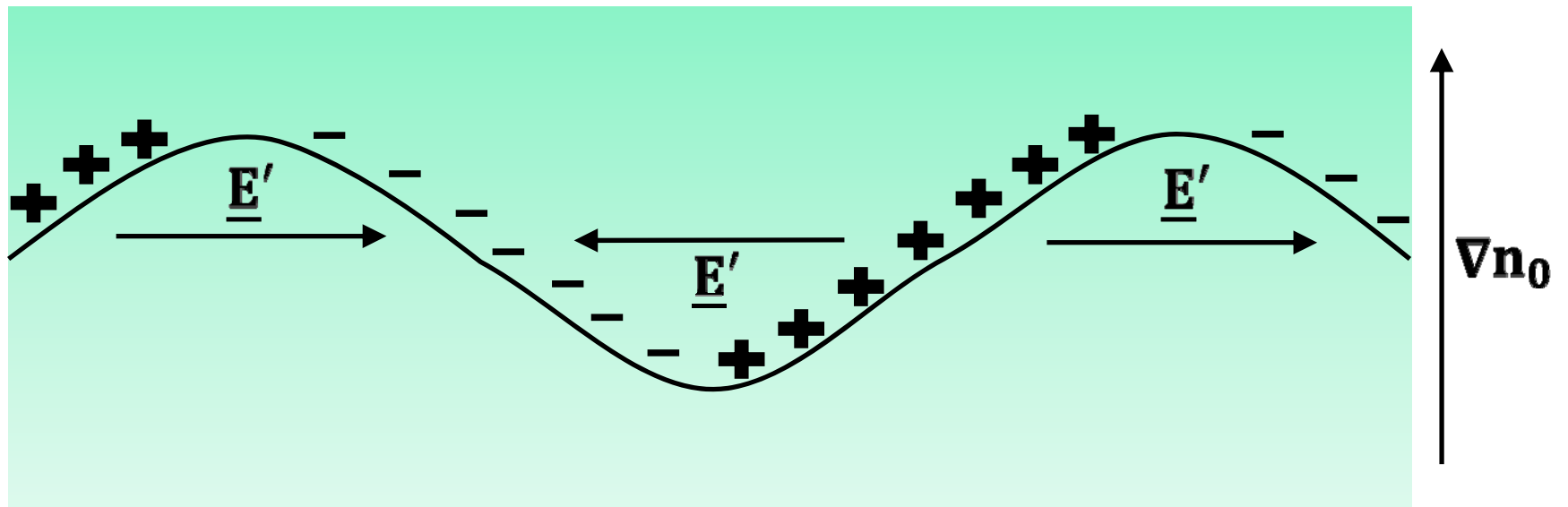


F region Gradient Drift Instability (GDI)

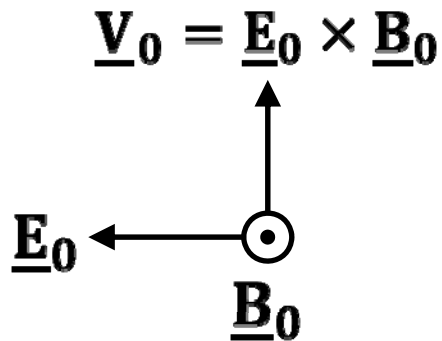
$$\underline{V}_0 = \underline{E}_0 \times \underline{B}_0$$

2. In the *F* region, the ions will drift to the left in the Pederson direction relative to the electrons, creating charge separation and small-scale polarization electric fields in alternating directions.

F Region Ionosphere

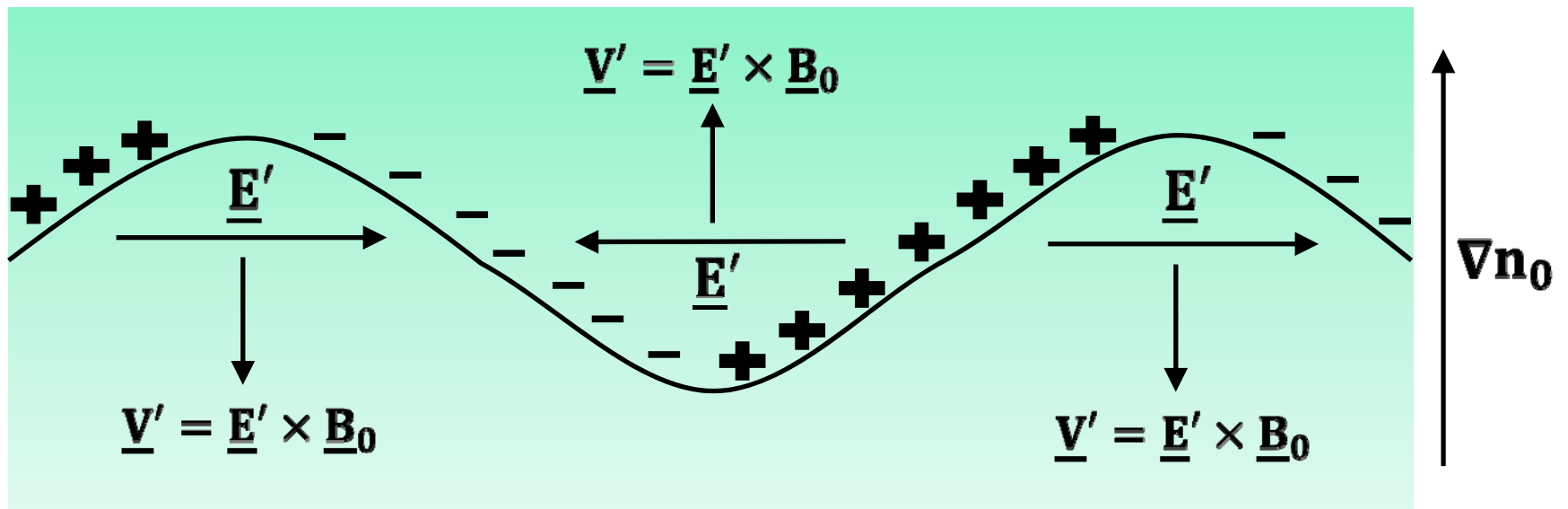


F region Gradient Drift Instability (GDI)



3. The resulting $\underline{E}' \times \underline{B}_0$ drifts will convect the enhanced plasma into regions of lower density and depleted plasma into regions of higher density, causing further destabilization [Keskinen and Ossakow, 1983].

F Region Ionosphere



An Experiment to Test the GDI Hypothesis

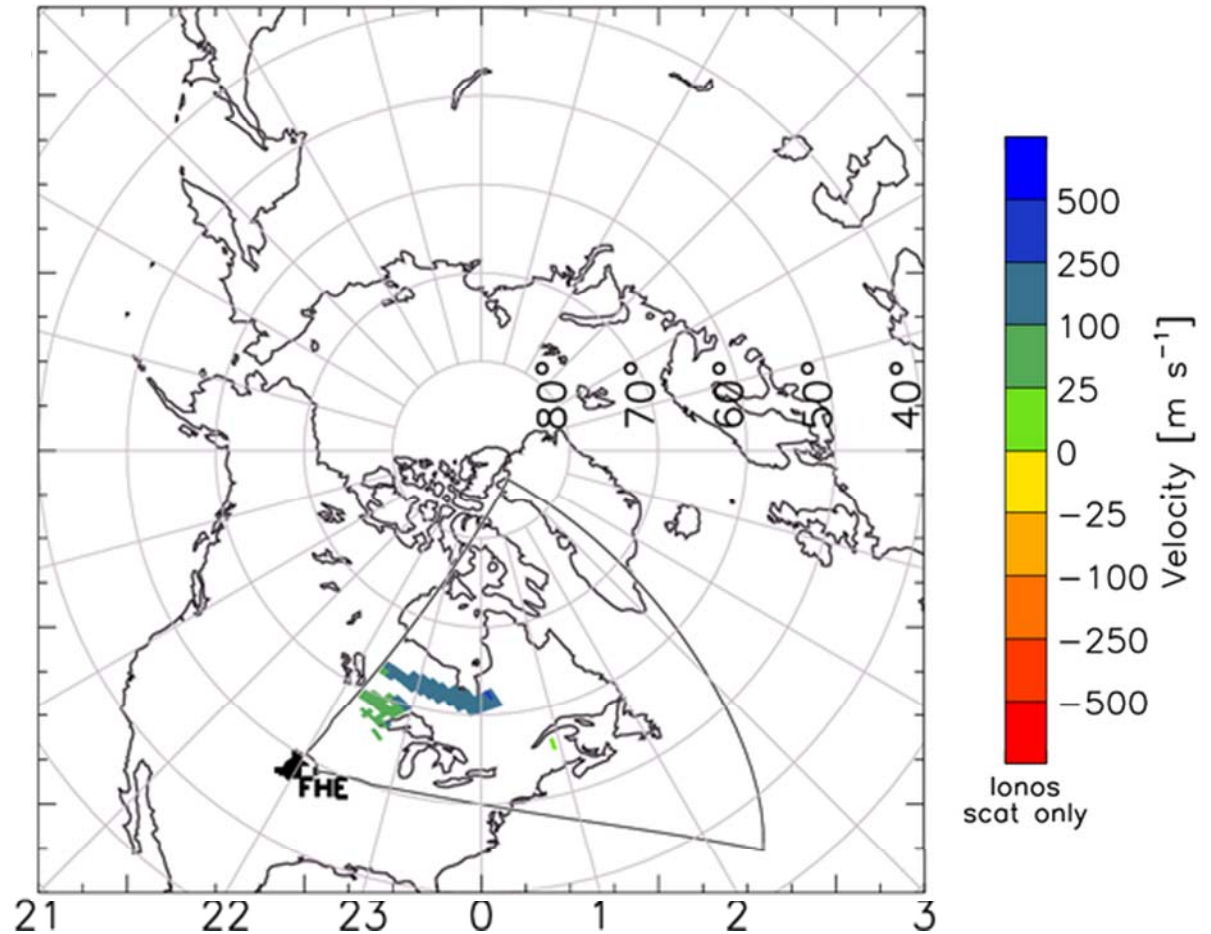
Question: What is the plasma instability mechanism that gives rise to the decameter-scale irregularities that make SAPS / Polar Jets visible to HF radar?

Consider – the F region gradient-drift instability, which requires a plasma velocity parallel to the plasma density gradient in the plane perpendicular to the magnetic field, i.e., $\mathbf{E} \times \mathbf{B} \parallel \text{grad } N_e$

Compare – data collected with SuperDARN radars, GPS/TEC measurements, and measurements of plasma properties from the Incoherent Scatter Radar (ISR) located at Millstone Hill Observatory (MHO)

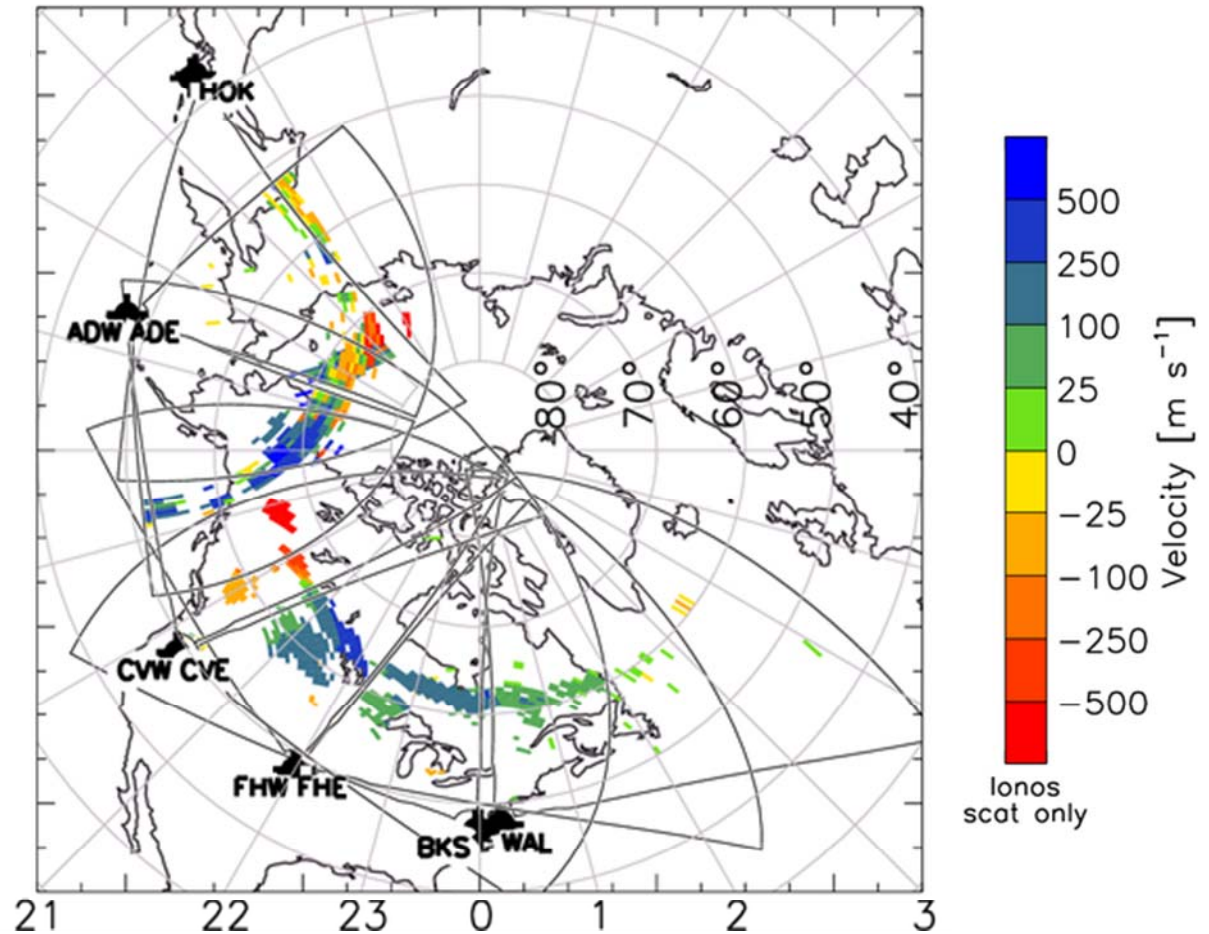
Observations of SAPS Channel – One radar

Subauroral polarization stream (SAPS) feature as seen by a single mid-latitude SuperDARN radar (Fort Hays East) at 05:00 UT on February 2nd, 2013.



Observation of SAPS Channel – Many radars

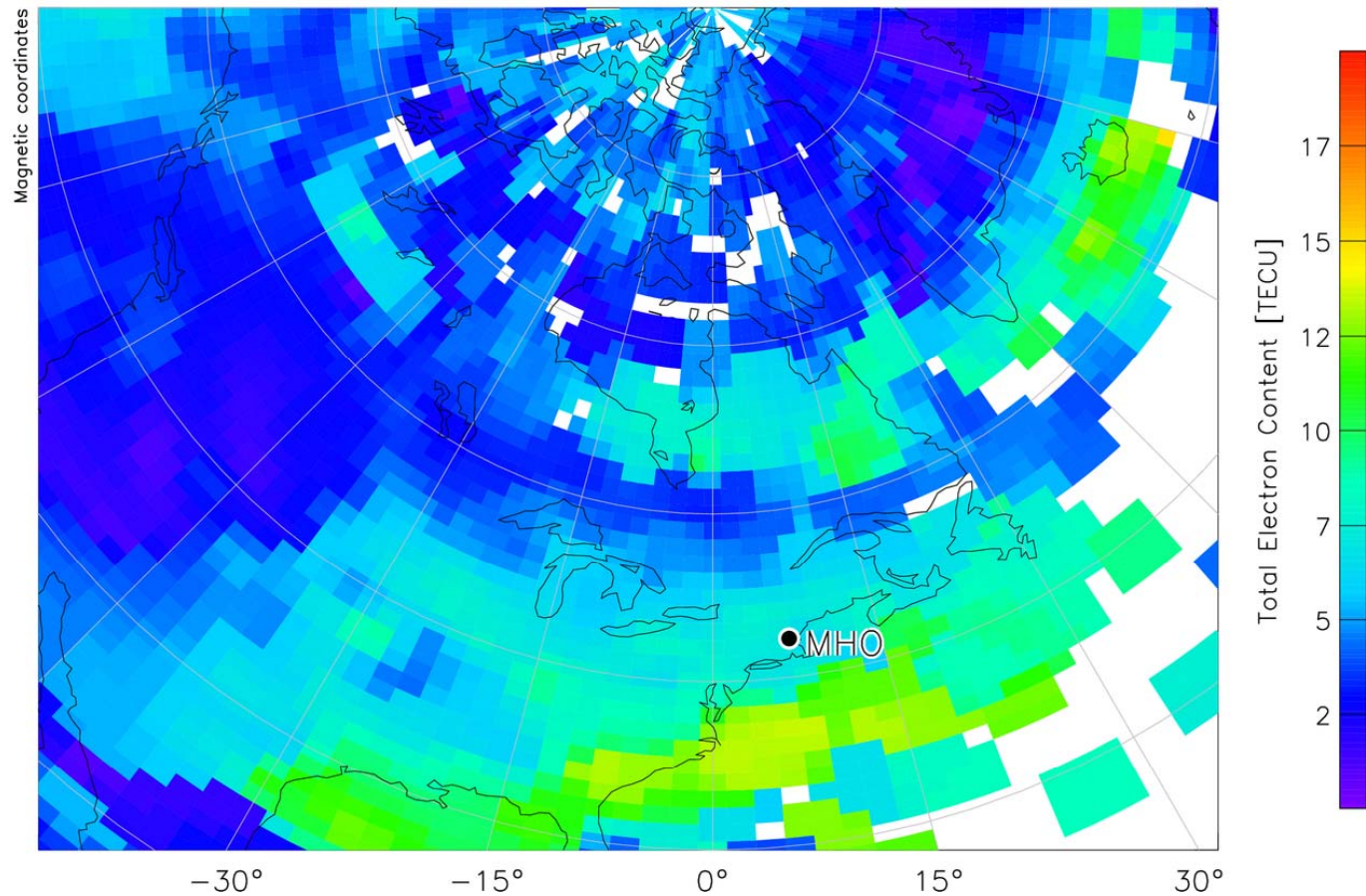
Subauroral polarization stream (SAPS) feature as seen by the full chain of mid-latitude SuperDARN radars at 05:00 UT on February 2nd, 2013.



Measurements of Total Electron Content from GPS

Feb 2 Trough
Map @ 04:41

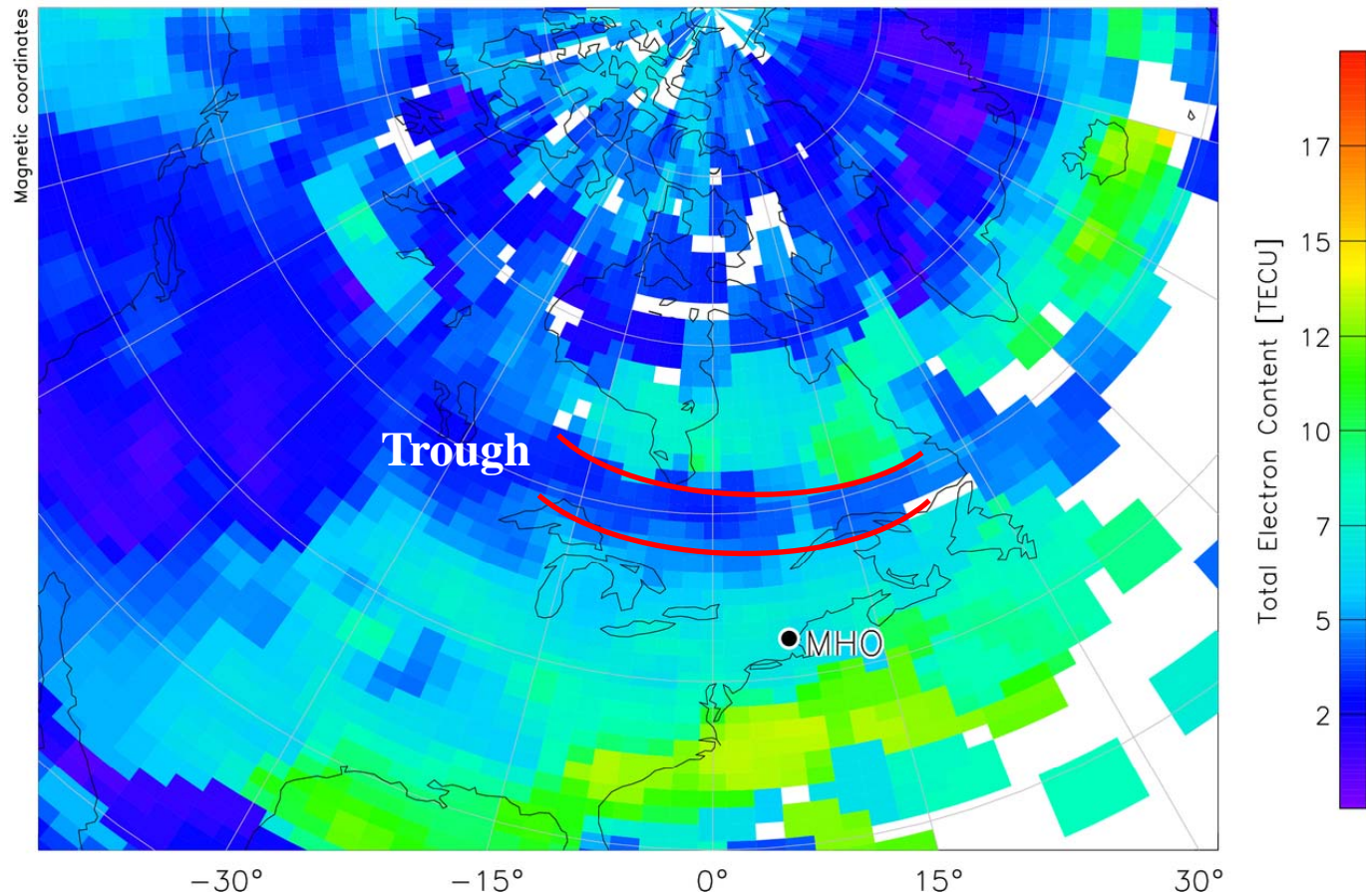
02/Feb/2013 04:40:33
to
02/Feb/2013 04:54:34



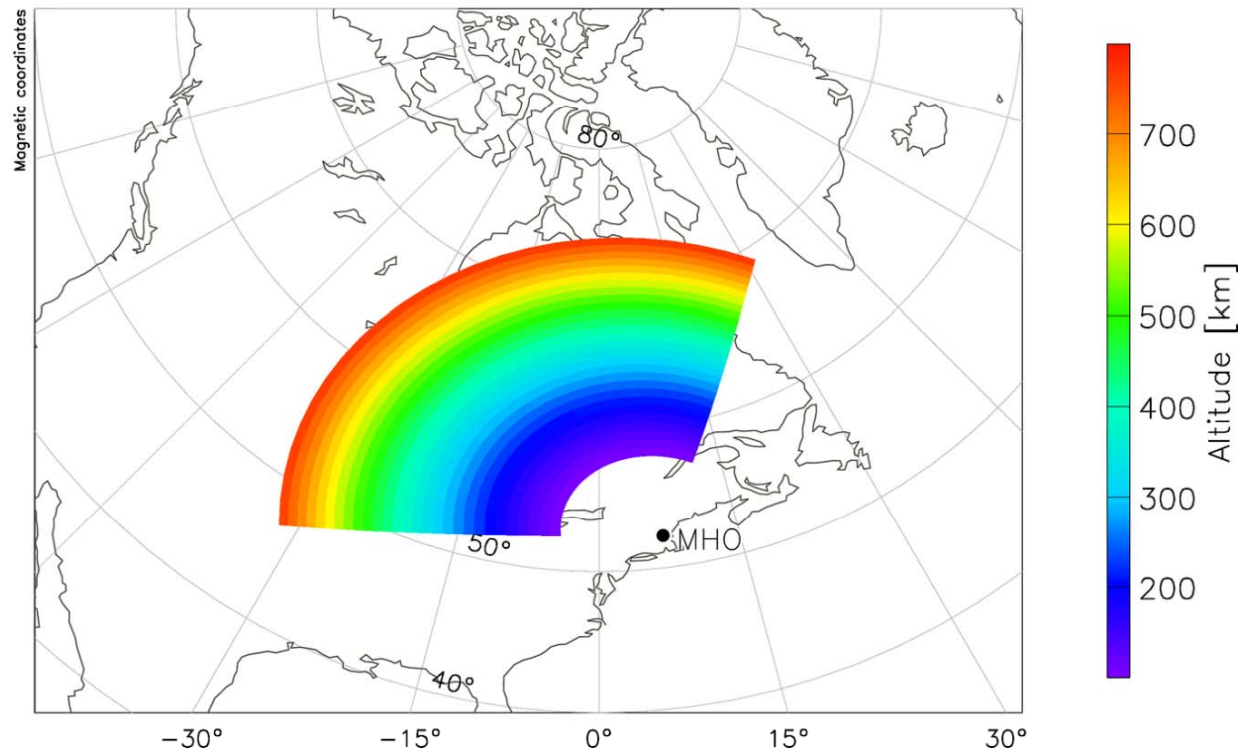
Measurements of Total Electron Content from GPS

Feb 2 Trough
Map @ 04:41

02/Feb/2013 04:40:33
to
02/Feb/2013 04:54:34



Perform Azimuthal Scanning with the ISR at MHO

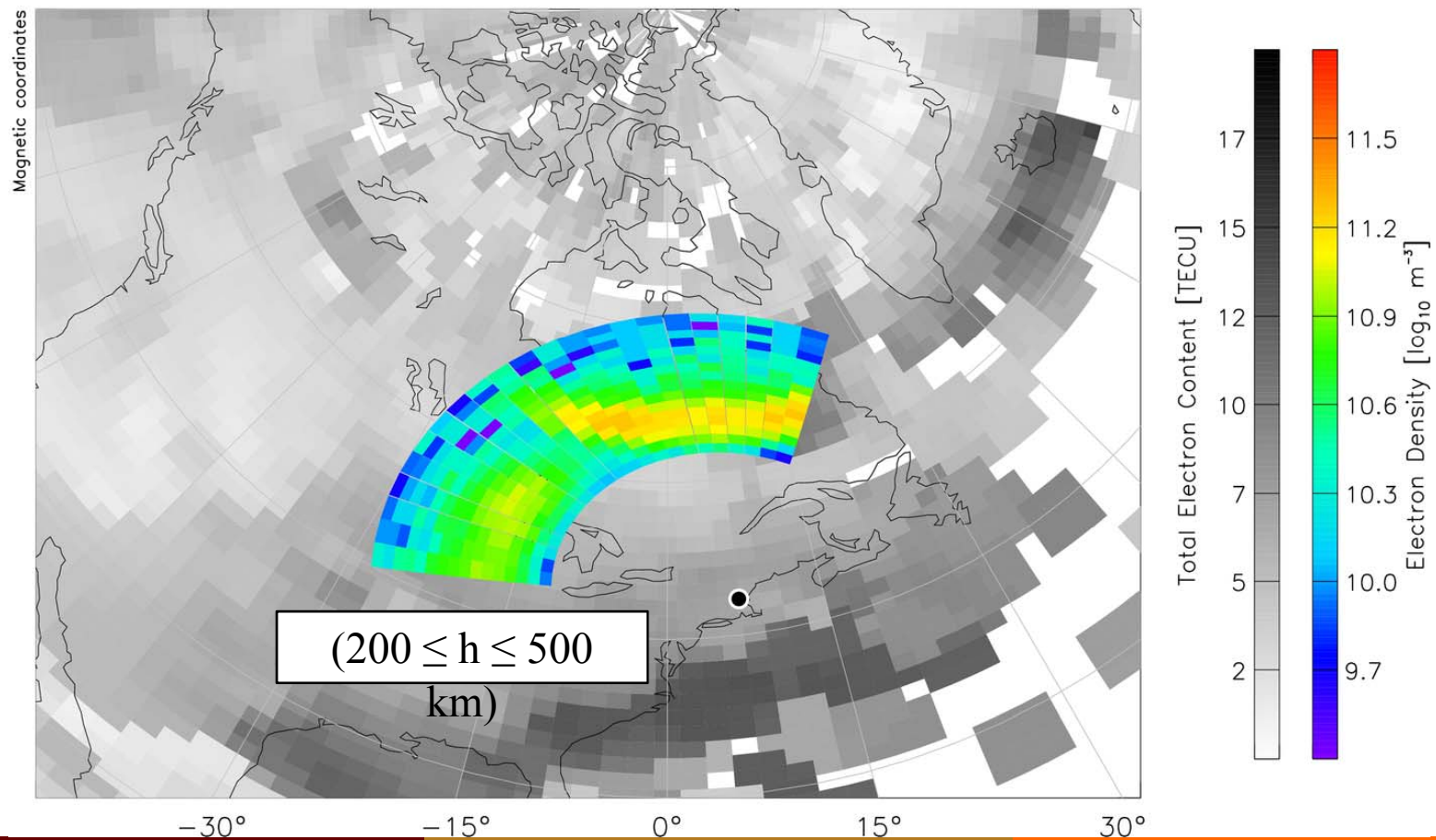


During this experiment the Millstone Hill Incoherent Scatter Radar (ISR) performed azimuth scans with a 6° elevation angle to measure ion/electron velocity, temperature, and density data at mid-latitudes over North America.

Electron Density from ISR Observations and TEC

Feb 2 Trough
Map @ 04:41

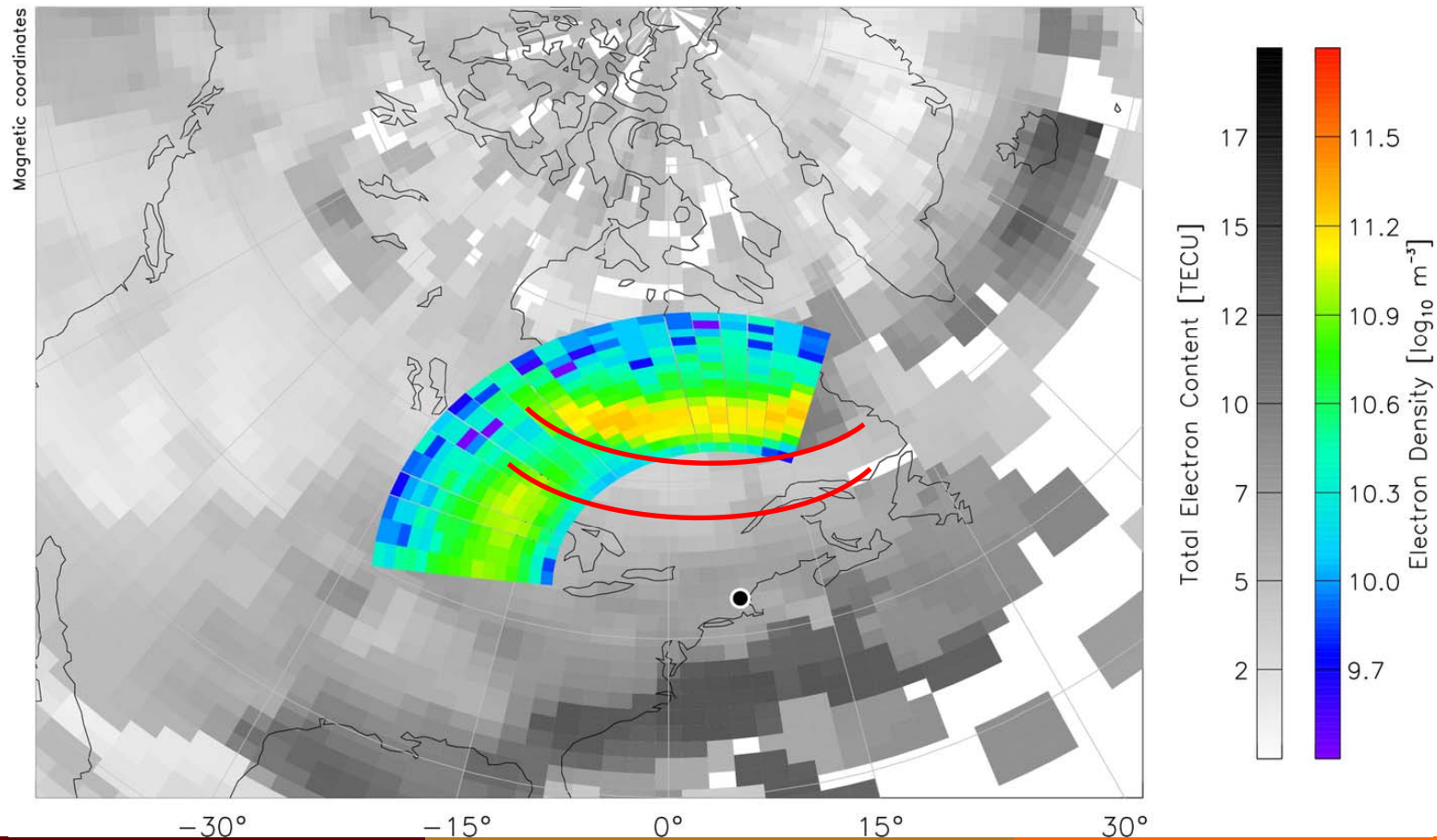
02/Feb/2013 04:40:33
to
02/Feb/2013 04:54:34



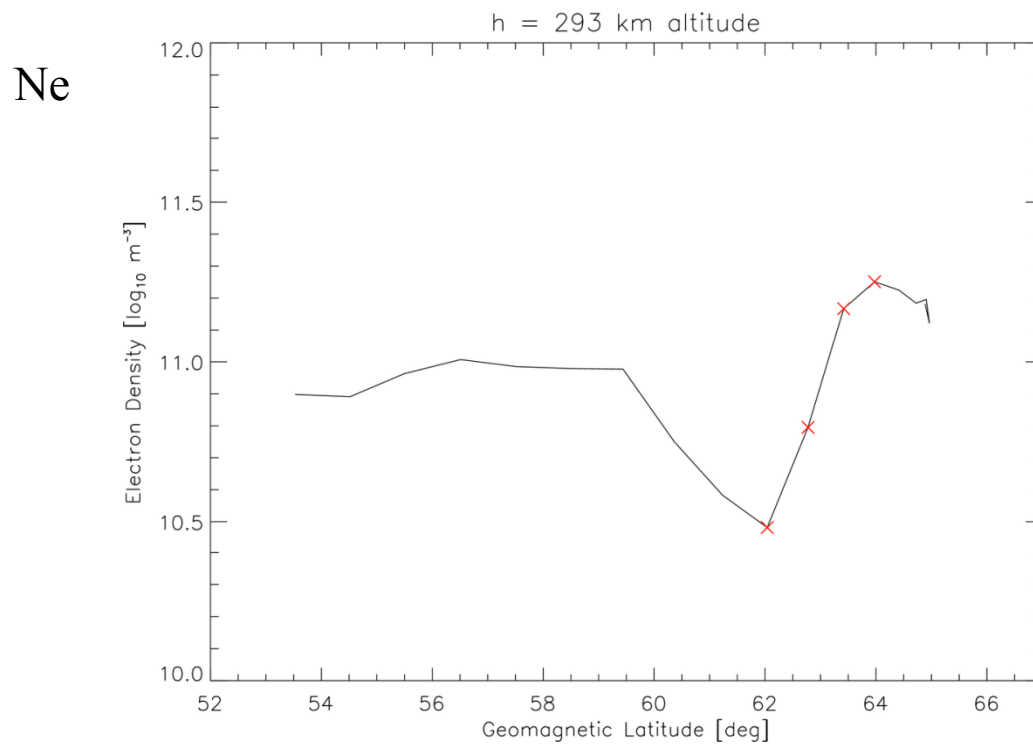
Identification of the trough in ISR and TEC data

Feb 2 Trough
Map @ 04:41

02/Feb/2013 04:40:33
to
02/Feb/2013 04:54:34



Ne versus Latitude (ISR)

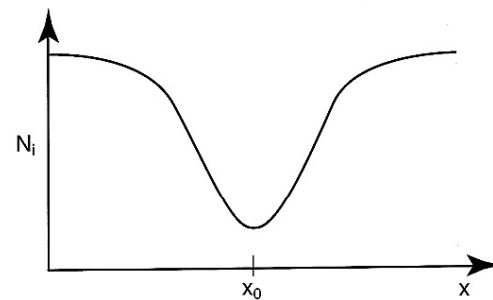


The ISR data indicate a classic plasma density trough with a very steep gradient at the poleward wall.

A component of $\mathbf{E} \times \mathbf{B}$ velocity in this direction would be favorable for the GDI.

Ne

Model Trough:
[Keskinen *et al.*, 2004]



Linear growth rate of GDI (fluid regime): Calculations

The linear growth rate of field-aligned irregularities (FAIs) from the gradient drift instability (GDI) in a collisional plasma in the fluid regime is given by:

$$\gamma_c \propto \frac{V_0}{L}$$

where $V_0 = \frac{E_0}{B}$ is the plasma velocity parallel to the density gradient and $L = \frac{n_0}{\nabla n_0}$ is the plasma density gradient scale length [Keskinen and Ossakow, 1983].

The complete linear expression includes a diffusion term which opposes the growth of FAIs:

$$\begin{aligned}\gamma_c &\propto \frac{V_0}{L} - k^2 D_{\perp} \\ &= \frac{E_0}{B} \cdot \frac{\nabla n_0}{n_0} - k^2 D_{\perp}\end{aligned}$$

where the plasma diffusion coefficient perpendicular to the magnetic field $D_{\perp} = 2D_{e\perp}$, and the electron diffusion coefficient is given by [e.g., Rishbeth and Garriott, 1969]:

$$D_{e\perp} = \frac{k_B T_e v_{ei} m_e}{e^2 B^2}$$

Linear growth rate of GDI (fluid regime): Calculations

Solving for the electron-ion collision frequency,

$$\nu_{ei} = \left[59 + 4.18 \log_{10} \left(T_e^3 / n_e \right) \right] n_e T_e^{-3/2} 10^{-6} = 24.51 \text{ s}^{-1}$$

Solving for the plasma diffusion coefficient,

$$D_{\perp} = \frac{2k_B T_e \nu_{ei} m_e}{e^2 B^2} = 0.0163 \text{ m}^2 \text{ s}^{-1}$$

Solving for the electron density gradient,

$$\nabla n_e = \frac{\partial n_e}{\partial y} = \frac{1.78 \times 10^{11} - 3.03 \times 10^{10}}{253 \times 10^3} = 5.85 \times 10^5 \text{ m}^{-4}$$

Solving for the wavenumber and minimum wavelength of unstable FAIs,

$$k_{crit} = \sqrt{\frac{1}{LD_{\perp}} \cdot \frac{E_0}{B}} = 0.2974$$

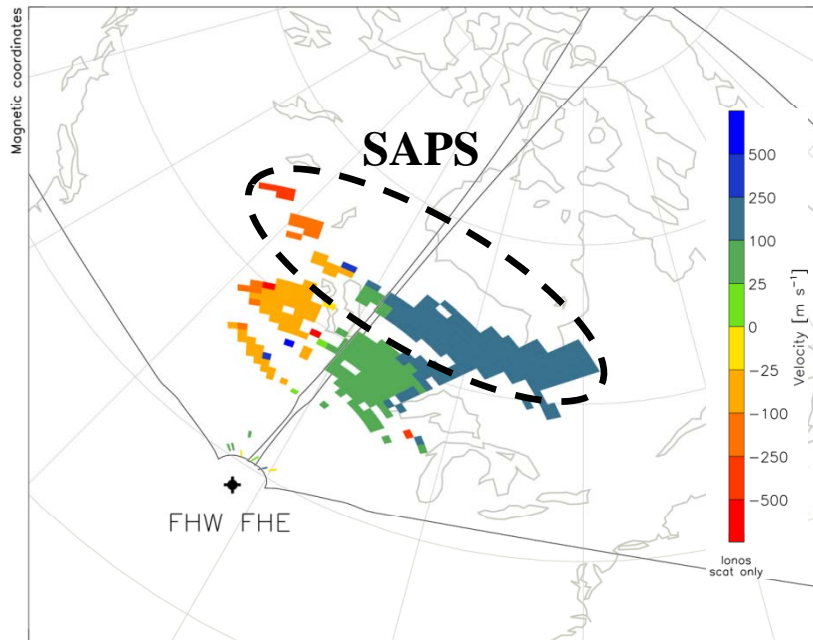
$$\lambda_{crit} = \frac{2\pi}{k_{crit}} = \frac{2\pi}{0.2974} \\ = 21 \text{ m}$$

$$V_0 \cong 75 \text{ m/s}$$

An Experiment to Test the GDI Hypothesis

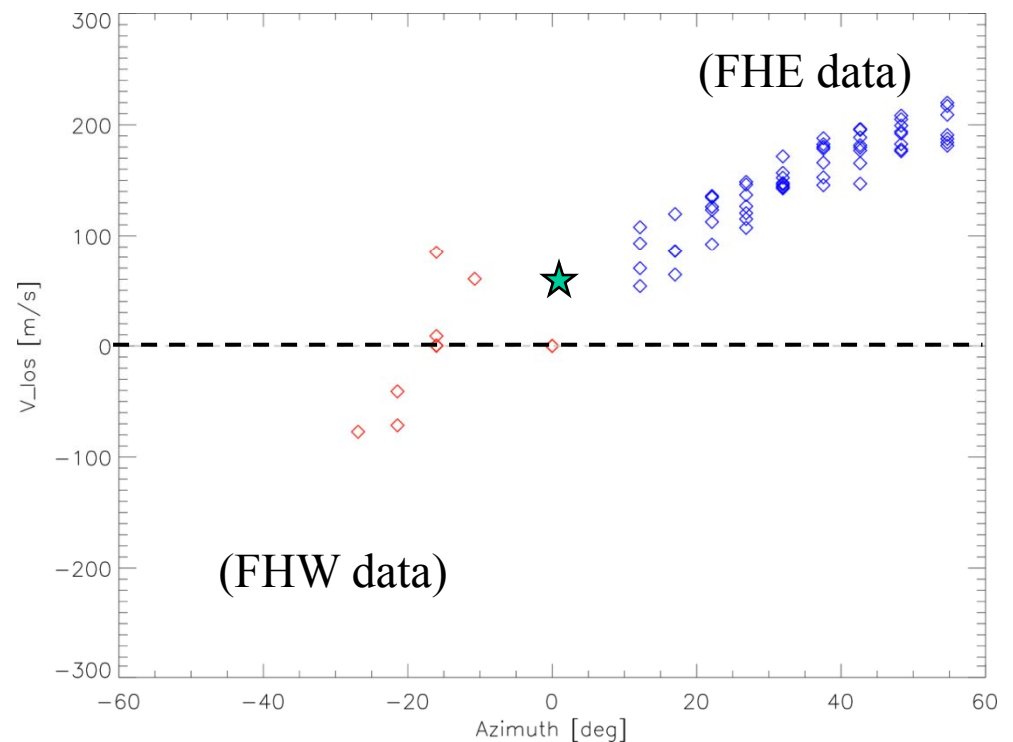
- We have determined that a plasma velocity of 75 m/s along the plasma density gradient at the poleward wall would destabilize the plasma at 10 m wavelengths by the GDI
- The SAPS $\mathbf{E} \times \mathbf{B}$ velocity is much larger than this, typically ~ 1 km/s...
- ...but it is primarily westward, not poleward
- Could there be a component in the poleward direction?
- Let's look more closely at the SuperDARN velocity data

SuperDARN Observations of SAPS Velocity



- Assuming the SAPS plasma drift is L-shell aligned, we can examine the LOS velocities as a function of azimuth to determine the N/S and E/W components.

- There is actually an equatorward velocity component observed within the SAPS channel, which is anti-parallel to ∇n_e



An Experiment to Test the GDI Hypothesis

- The \mathbf{ExB} velocity at the poleward wall is in the opposite direction for plasma instability by the GDI
- Instead, the GDI is stabilizing, it acts to decrease the plasma density fluctuations!
- We might consider other possibilities:
 - temperature gradient instability (TGI)
 - turbulent cascade from larger-scale irregularities
- The source of irregularities for coherent HF backscattering is very much an open research question

Summary: ‘Observations with ... SuperDARN HF Radar’

- The occurrence of coherent scattering from irregularities in the ionosphere is very useful for studies of plasma convection and magnetosphere-ionosphere coupling and for conducting experiments in plasma physics
- The scope for research in the physics of the mid-latitude ionosphere is increasing with the construction of HF coherent radars in the Russian sector
- There are many new research tools and open questions for young researchers to consider!

References

- For reviews of SuperDARN through its first and second decades see:

Chisham, et al., A decade of the Super Dual Auroral Radar Network (SuperDARN): Scientific achievements, new techniques and future directions, *Surveys in Geophysics*, 28, 33-109, doi:10.1007/s10712-007-9017-8, 2007

Greenwald, R.A., Baker, K.B., Dudeney, J.R., Pinnock, M., Jones, T.B., Thomas, E.C., Villain, J.-P., Cerisier, J.-C., Senior, C., Hanuise, C., Hunsucker, R.D., Sofko, G., Koehler, J., Nielsen, E., Pellinen, R., Walker, A.D., Sato, N., Yamagishi, H. DARN/SuperDARN: A global view of the dynamics of high latitude convection. *Space Sci. Rev.* 71, 761–796, 1995.

- For discussion of mid-latitude results see:

Clausen, L. B. N., J. B. H. Baker, J. M. Ruohoniemi, R. A. Greenwald, E. G. Thomas, S. G. Shepherd, E. R. Talaat, W. A. Bristow, Y. Zheng, A. J. Coster, and S. Sazykin, Large-scale observations of a subauroral polarization stream by midlatitude SuperDARN radars: Instantaneous longitudinal velocity variations, *J. Geophys. Res.*, 117, A05306, doi:10.1029/2011JA017232, 2012.

Ribeiro, A. J., J. M. Ruohoniemi, J. B. H. Baker, L. B. N. Clausen, R. A. Greenwald, and M. Lester, A survey of plasma irregularities as seen by the midlatitude Blackstone SuperDARN radar, *J. Geophys. Res.*, 117, A02311, doi:10.1029/2011JA017207, 2012

de Larquier, S., P. Ponomarenko, A. J. Ribeiro, J. M. Ruohoniemi, J. B. H. Baker, K. T. Sterne, and M. Lester (2013), On the spatial distribution of decameter-scale subauroral ionospheric irregularities observed by SuperDARN radars, *J. Geophys. Res. Space Physics*, 118, 5244–5254, doi:10.1002/jgra.50475

- For discussion of plasma instabilities see:

de Larquier, S., A. Eltrass, A. Mahmoudian, J. M. Ruohoniemi, J. B. H. Baker, W. A. Scales, P. J. Erickson, and R. A. Greenwald (2014), Investigation of the temperature gradient instability as the source of midlatitude quiet time decameter-scale ionospheric irregularities: 1. Observations, *J. Geophys. Res. Space Physics*, 119, 4872–4881, doi:10.1002/2013JA019643

Eltrass, A., A. Mahmoudian, W. A. Scales, S. de Larquier, J. M. Ruohoniemi, J. B. H. Baker, R. A. Greenwald, and P. J. Erickson (2014), Investigation of the temperature gradient instability as the source of midlatitude quiet time decameter-scale ionospheric irregularities: 2. Linear analysis, *J. Geophys. Res. Space Physics*, 119, 4882–4893, doi:10.1002/2013JA019644

References

- For first papers from the Ekaterinburg HF radar:

Berngardt, O. I., A. L. Voronov, and K. V. Grkovich (2015), Optimal signals of Golomb ruler class for spectral measurements at EKB SuperDARN radar: Theory and experiment, *Radio Sci.* , 50, 486–500. doi:10.1002/2014RS005589

Mager, P. N., O. I. Berngardt, D. Y. Klimushkin, N. A. Zolotukhina, O. V. Mager (2015), First results of the high-resolution multibeam ULF wave experiment at the Ekaterinburg SuperDARN radar: Ionospheric signatures of coupled Alfvén and drift-compressional modes, *J. Atmos. Terrest. Phys.*, 130-131, pp. 112-126, doi:10.1016/j.jastp.2015.05.017.

The author on the grounds of the Siberian Radio Telescope (SSRT) located at Badary with the Eastern Sayan mountains in the background.

The SSRT is operated by the ISTP SB RAS.

Photo: Courtesy of Nosikov Igor

